REVISED

Supporting Information for:

Synthesis of Meso-Substituted Chlorins via Tetrahydrobilene-*a* Intermediates

Masahiko Taniguchi, Doyoung Ra, Guoning Mo, Thiagarajan Balasubramanian,

and Jonathan S. Lindsey*

Isolation of an Iodinated Product During the Attempted Synthesis of a Chlorin.

During our initial synthesis of a chlorin using the tetrahydrodipyrrin Western half, we employed the condensation and oxidation conditions[1] developed for the dipyrrin Western half (SI Scheme 1). Thus, a reaction was performed of **4** and an iodo-phenyl substituted Eastern half (**6g-OH**) in acetonitrile containing 10 mM TFA followed by oxidative cyclization using $AgIO_3$, $Zn(OAc)_2$, and piperidine in toluene at 80 °C. In addition to the desired chlorin (**Zn-8h**), we identified a byproduct upon examination of the LD-MS spectrum. The LD-MS spectrum shows peaks at m/z = 694 and 820, the former of which corresponds to the desired chlorin (**Zn-8h**). This Δm of 126 is ascribed to the presence of an iodo atom (note that the chlorin target molecule **Zn-8h** bears a single iodo group; the byproduct bears two iodo groups). However, only a single chlorin spot was observed upon TLC analysis. The absorption spectrum in the $Q_y(0,0)$ region was somewhat broad. Upon demetalation of the zinc-chlorin material, TLC analysis showed the presence of two chlorin species. Isolation and characterization (particularly with ^{1}H NMR and NOE experiments) revealed that the iodination occurred regiospecifically at the 2-position. We note that this iodinated byproduct may have useful synthetic applications. The following experimental section describes the isolation and characterization of the 2-iodo-chlorin byproduct. The yield following demetalation of the zinc chlorins was 12% (desired chlorin **Fb-8g**) and 6% (iodo-chlorin byproduct **Fb-8h**).

Synthesis of 17,18-dihydro-10-(4-iodophenyl)-18,18-dimethyl-5-(4-methylphenyl)-porphyrin (Fb-8g) and 17,18-dihydro-2-iodo-10-(4-iodophenyl)-18,18-dimethyl-5-(4-methylphenyl)porphyrin (Fb-8h). Following the general procedure,[1] treatment of **6g** (272 mg, 0.500 mmol) with $NaBH_4$ (114 mg, 3.01 mmol) in 7.5 mL of anhydrous THF/methanol (4:1) afforded **6g-OH**. After removal of the solvent, the residue was dissolved in 50 mL of anhydrous CH_3CN. A sample of **4** (100 mg, 0.530 mmol) was added followed by TFA (38 μL, 0.50 mmol, 10 mM). The solution was stirred at room temperature for 30 min. The reaction was quenched with 10% aqueous $NaHCO_3$ (50 mL) and extracted with distilled CH_2Cl_2 (3 × 50 mL). The combined organic layers were washed with water, dried (Na_2CO_3) and concentrated in vacuo without heating. The residue was dissolved in 50 mL of toluene, to which $AgIO_3$ (2.12 g, 7.50 mmol), $Zn(OAc)_2$ (1.38 g, 7.50 mmol) and piperidine (740 μL, 7.50 mmol) were added. The reaction mixture was heated at 80 °C exposed to air for 2 h. The reaction mixture was concentrated under reduced pressure. The residue was passed through a short silica gel column eluting with CH_2Cl_2. The major fraction was concentrated and again chromatographed [silica, hexanes/CH_2Cl_2 (2:1)] to afford a blue solid (66 mg). From the blue solid, 56 mg was taken and dissolved in 10 mL of CH_2Cl_2 and treated with TFA (310 μL, 4.04 mmol). The demetalation was complete in 1 h as confirmed by UV-Vis and TLC analyses. Then 70 mL of CH_2Cl_2 and 2 mL of triethylamine were added to the reaction mixture. The mixture was washed with saturated aqueous $NaHCO_3$ (2 × 100 mL) and dried (Na_2SO_4). TLC analysis [silica, hexanes/CH_2Cl_2 (1:1)] showed two components [R_f = 0.72, **Fb-8h**; R_f = 0.57, **Fb-8g**]. The solvent was removed under vacuum. Chromatography of the residue [silica, hexanes/CH_2Cl_2 (3:1)] afforded **Fb-8g** (32 mg, 12%) and **Fb-8h** (19 mg, 6%). Analytical data of **Fb-8g** were consistent with literature values.[1] **Fb-8h**: ^{1}H NMR δ –1.66 (bs, 2H), 2.07 (s, 6H), 2.67 (s, 3H), 4.58 (s, 2H), 7.51 (d, J = 8.1 Hz, 2H), 7.82 (d, J = 8.1 Hz, 2H), 7.96 (d, J = 8.1 Hz, 2H), 8.03 (d, J = 8.1 Hz, 2H), 8.40 (d,

J = 4.4 Hz, 1H, H_8), 8.48 (d, J = 4.4 Hz, 1H, H_7), 8.70 (d, J = 4.4 Hz, 1H, H_{12}), 8.77 (d, J = 4.4 Hz, 1H, H_{13}), 8.88 (s, 1H, H_{20}), 8.95 (s, 1H, H_{15}), 8.97 (s, 1H, H_3); LD-MS obsd 757.24; FAB-MS obsd 759.0480, calcd 759.0482 ($C_{35}H_{28}I_2N_4$); λ_{abs} (toluene) 420, 512, 649 nm.

Possible Oxidized Intermediates Formed During Metal-Mediated Oxidative Cyclization.

Spectral monitoring of the conversion of the tetrahydrobilene-*a* to the chlorin (Figure 3, main text) shows the appearance and disappearance of a band at 505 nm. Scheme 3 (main text) shows a series of processes for conversion of the tetrahydrobilene-*a* to the chlorin. We emphasize that Scheme 3 illustrates formal processes and the actual process is expected to be more complex. Indeed, the oxidation process requires the removal of six electrons and six protons; no intermediate oxidation products are shown in Scheme 3. It is likely that a dipyrrin chromophore formed upon oxidation is complexed with zinc, yielding the observed band at 505 nm. The structure of this complex is not known. To our knowledge, all zinc-dipyrrins that have been reported incorporate two dipyrrins per zinc atom.[2] The absorption spectra of a variety of bis(dipyrrinato)zinc(II) complexes show maxima in the 500-nm region.

SI Scheme 2 shows several zinc dipyrrin chromophores which are putative intermediates in the conversion of the tetrahydrobilene-*a* to the chlorin. The existence of the band at 505 nm suggests that oxidation and complexation processes are interspersed rather than occurring sequentially as displayed in the formal rendering in Scheme 3.

- Consider first the products formed upon two-electron, two-proton oxidation. Inspection of SI Scheme 2 shows that there are no zinc-chelated bis(dipyrrin) structures that can be derived by intramolecular complexation of a single tetrapyrrolic structure. Considering only intramolecular complexation of a tetrapyrrolic structure, there are two possible zinc-chelated dipyrrins (**A**, **B**) both of which would require an anionic counterion to compensate the zinc

dication. The expected absorption bands of these structures are not known, especially due to the presence of the α-bromo substituent, nor is the absorption spectrum known for the zinc-dihydrodipyrrin (**C**). Noteworthy spectral landmarks are as follows: (1) The absorption spectrum of bis(1,9-dibromo-5-phenyldipyrrinato)zinc(II) exhibited λ_{max} = 500 nm in toluene and λ_{max} = 498 nm in CH_2Cl_2/pyridine.[3] (2) The absorption spectrum of a 2,3,4,5-tetrahydrobiladiene-*ac* incorporating an α-bromo-dipyrrin unit with a full complement of β-substituents exhibited λ_{max} = 494 nm in CH_2Cl_2. The addition of $Cu(OAc)_2$ in DMF and methanol gave the copper chelate with λ_{max} = 508 nm.[4]

- Turning to the products formed upon four-electron, four-proton oxidation, there again are no zinc-chelated bis(dipyrrin) structures that can be formed of a single tetrapyrrolic structure. The absorption spectra of structures such as the mixed dipyrrin-dihydrodipyrrin complex (**D**), the tripyrrin complex (**E**), or the dihydrotripyrrin complex (**F**) are not known. While **D** comprises both a dipyrrin and a dihydrodipyrrin ligand in one tetrapyrrole, the structure is unlikely to be able to assume a tetrahedral geometry about the zinc ion.
- Finally, the six-electron, six-proton oxidized system (**G**) as shown requires an anionic counterion to compensate the zinc dication, though upon formation of the enamine tautomer the counterion would not be required.

Consideration of these structures reveals that the only way to achieve the normal zinc-chelated bis(dipyrrin) structures with oxidized products from the tetrahydrobilene-*a* is by complexation of two tetrapyrrolic structures each of which has undergone two-electron, two-proton oxidation. Such structures are not displayed in SI Scheme 2. While zinc-chelated bis(dipyrrin) structures derived from two tetrapyrrolic units are possible intermediates, such species cannot lead directly to chlorin formation. Much more work is required to characterize the intermediates formed during the conversion of the tetrahydrobilene-*a* to the chlorin.

Results from the Attempted Metal-Mediated Oxidative Cyclization Employing Quinones.

We initially examined the use of various quinones in the metal-mediated oxidation process before arriving at the refined conditions described in the main text. Using *p*-chloranil, piperidine, and $Zn(OAc)_2$, chlorin **Zn-8a** was isolated in yields of 4-15% upon reaction in various solvents (THF, toluene, or dichloromethane) at a range of temperatures (room temperature to 80 °C) for reaction times from 1 to 5 h. Under these conditions, two distinct byproducts (**Zn-8a′**, **Zn-8a″** in order of chromatographic elution) were formed in yields of up to ~25% each. Each byproduct upon purification exhibited the following spectra data: (1) one meso-proton of the chlorin was missing in the ^{1}H-NMR spectrum; (2) the LD-mass spectrum showed a peak at m/z = 866 or 820 for **Zn-8a′** or **Zn-8a″**, respectively; (3) the long-wavelength absorption band in the UV/vis spectrum was slightly red-shifted (611 or 612 nm) compared with that of the target chlorin (λ_{max} = 609 nm). All attempts to decrease the formation of these byproducts were unsuccessful. The byproducts **Zn-8a′** and **Zn-8a″** are assigned to the covalent chlorin-hydroquinone adducts as shown in SI Chart 1. In neither case were any atropisomers observed upon TLC analysis, though the presence of atropisomers was manifest in the ^{1}H NMR spectrum. The site of substitution has been identified through use of ^{1}H NMR spectroscopy and NOE experiments. The structure of **Zn-8a″** suggests a mechanism of electrophilic aromatic substitution on the chlorin macrocycle with displacement of chloride from the quinone followed by reduction yielding the hydroquinone. The structure of **Zn-8a′** shows attack of two species on the *p*-chloranil nucleus, the chlorin and piperidine. While 2,6- and 2,5-substitution patterns are equally likely (and cannot be distinguished based on the data in hand), there is precedence for the formation of 2,5-substitution products upon substitution and addition reactions of quinones with

pyrroles.[5] Note that when the reaction was performed with 2,2,6,6-tetramethylpiperidine instead of piperidine, the byproduct **Zn-8a″**, but not **Zn-8a′**, was formed.

Attempts to use other quinones also did not provide clean oxidations. With quinones such as DDQ, decomposition occurred; with *p*-benzoquinone, the chlorin and uncharacterized byproducts were obtained; with sterically hindered quinones such as 2,5-di-*tert*-butyl-*p*-benzoquinone or duroquinone in the presence of additives (e.g., AgTf, $AgBF_4$), the desired chlorin was obtained in yields of 60-70% without chlorin byproducts detected by LD-MS analysis. However, we subsequently found that in the latter case oxidation occurred due to exposure to air rather than by reaction with the quinone.

The procedure for chlorin formation using *p*-chloranil, exemplified for Zn(II)-17,18-dihydro-10-mesityl-18,18-dimethyl-5-(4-methylphenyl)porphyrin (Zn-8a). A solution of tetrahydrobilene **7a** (63.6 mg, 0.100 mmol) in toluene (10 mL) was treated with $Zn(OAc)_2$ (275 mg, 1.50 mmol) and *p*-chloranil (148 mg, 0.600 mmol) at room temperature for 75 min. Then piperidine (150 μL, 1.51 mmol) was added. The reaction mixture was stirred at room temperature for 1 h. Then the reaction mixture was refluxed for 2 h and 15 min. The reaction mixture was concentrated under reduced pressure, and the resulting residue was chromatographed [silica, hexanes/CH_2Cl_2 (1:1)] to give **Zn-8a** (8.9 mg, 15%) from the first band as a blue solid. After that two additional bands were obtained, affording a greenish-blue solid (**Zn-8a′**, 12.0 mg, 14%) and a greenish-blue solid (**Zn-8a″**, 20.9 mg, 25%). Analytical data for **Zn-8a** were consistent with literature values.[1] **Zn-8a′**: TLC analysis (silica, CH_2Cl_2, R_f = 0.68); ^{1}H NMR ($CDCl_3$) δ 1.64–1.83 (m, 10H), 1.83 (s, 3H), 1.87 (s, 3H), 1.96 (s, 3H), 1.99 (s, 3H), 2.56 (s, 3H), 2.65 (s, 3H), 3.20–3.40 (m, 4H), 3.44–3.72 (m, 6H), 3.97 (d, *J* = 16.9 Hz, 1H), 4.19 (d, *J* = 16.9 Hz, 1H), 5.75–5.98 (br, 2H), 7.16–7.19 (m, 2H), 7.45–7.51 (m, 2H), 7.88–7.99 (m, 2H), 8.13 (d, *J* = 4.4 Hz, 1H), 8.17 (d, *J* = 4.4 Hz, 1H), 8.29 (d, *J* = 4.4 Hz, 1H), 8.39 (d, *J* = 4.4

Hz, 1H), 8.48 (s, 1H), 8.58 (d, J = 4.4 Hz, 1H), 8.62 (d, J = 4.4 Hz, 1H); LD-MS obsd 866.40; FAB-MS obsd 869.2240, calcd 869.2242 ($C_{49}H_{45}Cl_2N_5O_2Zn$); λ_{abs} (toluene) 414, 611 nm.

Zn-8a″: TLC analysis (silica, CH_2Cl_2, R_f = 0.46); ^{1}H NMR ($CDCl_3$) δ 1.85 (s, 3H), 1.87 (s, 3H), 1.94 (s, 3H), 1.97 (s, 3H), 2.57 (s, 3H), 2.66 (s, 3H), 3.97 (s, 2H), 5.70–6.05 (br, 2H), 7.16–7.20 (m, 2H), 7.46–7.51 (m, 2H), 7.91–7.95 (m, 1H), 7.94–7.98 (m, 2H), 8.19 (d, J = 4.4 Hz, 1H), 8.32 (d, J = 4.4 Hz, 1H), 8.38 (d, J = 4.4 Hz, 1H), 8.50 (s, 1H), 8.60 (d, J = 4.4 Hz, 1H), 8.65 (d, J = 4.4 Hz, 1H); LD-MS obsd 819.59; FAB-MS obsd 820.1117, calcd 820.1103 ($C_{44}H_{35}Cl_3N_4O_2Zn$); λ_{abs} (toluene) 415, 612 nm.

Nomenclature of Tetrapyrrole Intermediates in Chlorin Syntheses.

We have employed the I.U.P.A.C. system of nomenclature for bilane derivatives,[6] as shown in SI Chart 2. Note that the 2,3-dihydrobilene has the same oxidation level as a bilane, whereas a 2,3,4,5-tetrahydrobilene has the same oxidation level as a dihydrobilane. We have employed the same nomenclature for chlorins as used previously.[7]

References.

(1) Strachan, J. P.; O'Shea, D. F.; Balasubramanian, T.; Lindsey, J. S. *J. Org. Chem.* **2000**, *65*, 3160-3172.

(2) (a) Granick, S.; Gilder, H. In *Advances in Enzymology*; Nord, F. F. Ed.; Interscience: New York, 1947; Vol. 7, pp 358-363. (b) Johnson, A. W.; Kay, I. T.; Markham, E.; Price, R.; Shaw, K. B. *J. Chem. Soc.* **1959**, 3416-3424. (c) Motekaitis, R. J.; Martell, A. E. *Inorg. Chem.* **1970**, *9*, 1832-1839. (d) March, F. C.; Couch, D. A.; Emerson, K.; Fergusson, J. E.; Robinson, W. T. *J. Chem. Soc. (A)* **1971**, 440-448. (e) Murakami, Y.; Matsuda, Y.; Kobayashi, S. *J. Chem. Soc. Dalton Trans.* **1973**, 1734-1737. (f) Hill, C.

L.; Williamson, M. M. *J. Chem. Soc., Chem. Commun.* **1985**, 1228-1229. (g) Brückner, C.; Karunaratne, V.; Rettig, S.; Dolphin, D. *Can. J. Chem.* **1996**, *74*, 2182-2193.

(3) Supporting information, reference 1.

(4) Battersby, A. R.; Fookes, C. J. R.; Snow, R. J. *J. Chem. Soc. Perkin Trans. 1* **1984**, 2725-2732.

(5) (a) Pratesi, P. *Gazz. Chim. Ital.* **1936**, *66*, 215-223. (b) Karius, H.; Mapstone, G. E. *Chem. Ind.* **1956**, 266-267. (c) Bullock, E. *Can J. Chem.* **1958**, *36*, 1744. (d) Fischer, H.; Treibs, A.; Zaucker, E. *Chem. Ber.* **1959**, *92*, 2026-2029. (e) Kuser, P.; Frauenfelder, E. F.; Eugster, C. H. *Helv. Chim. Acta* **1971**, 54, 969-979. (f) Kowalik, J.; Nguyen, H. T.; Tolbert, L. M. *Syn. Metals* **1991**, 435-438.

(6) Moss, G. P. *Pure Appl. Chem.* **1987**, *59*, 779-832.

(7) See supporting information: Balasubramanian, T; Strachan, J.-P.; Boyle, P. D.; Lindsey, J. S. *J. Org. Chem.* **2000**, *65*, 7919-7929.

SI Scheme 1

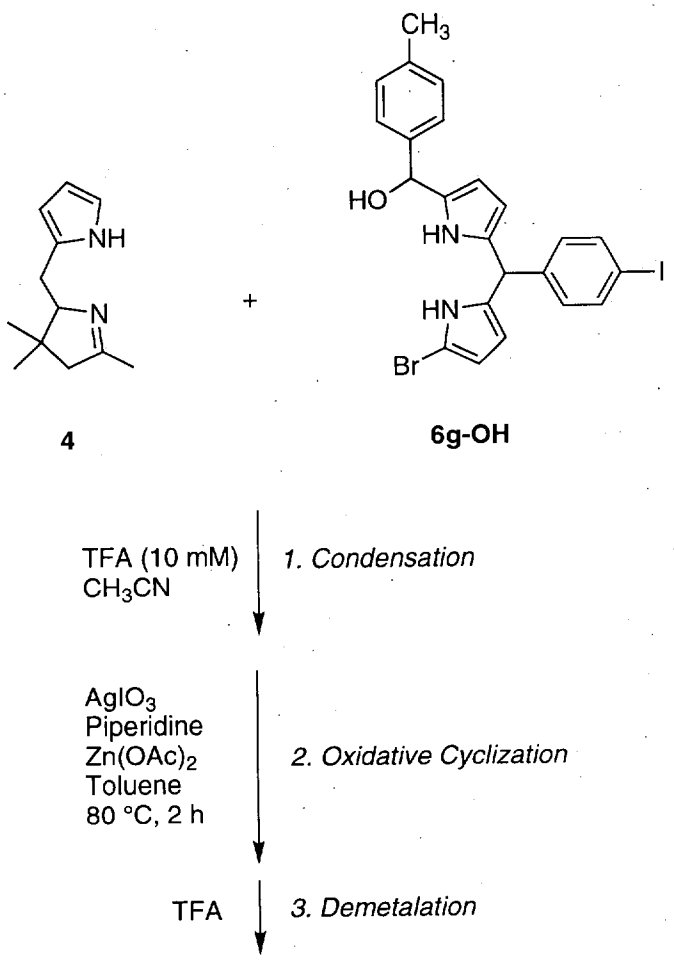

4 **6g-OH**

Fb-8g **Fb-8h**

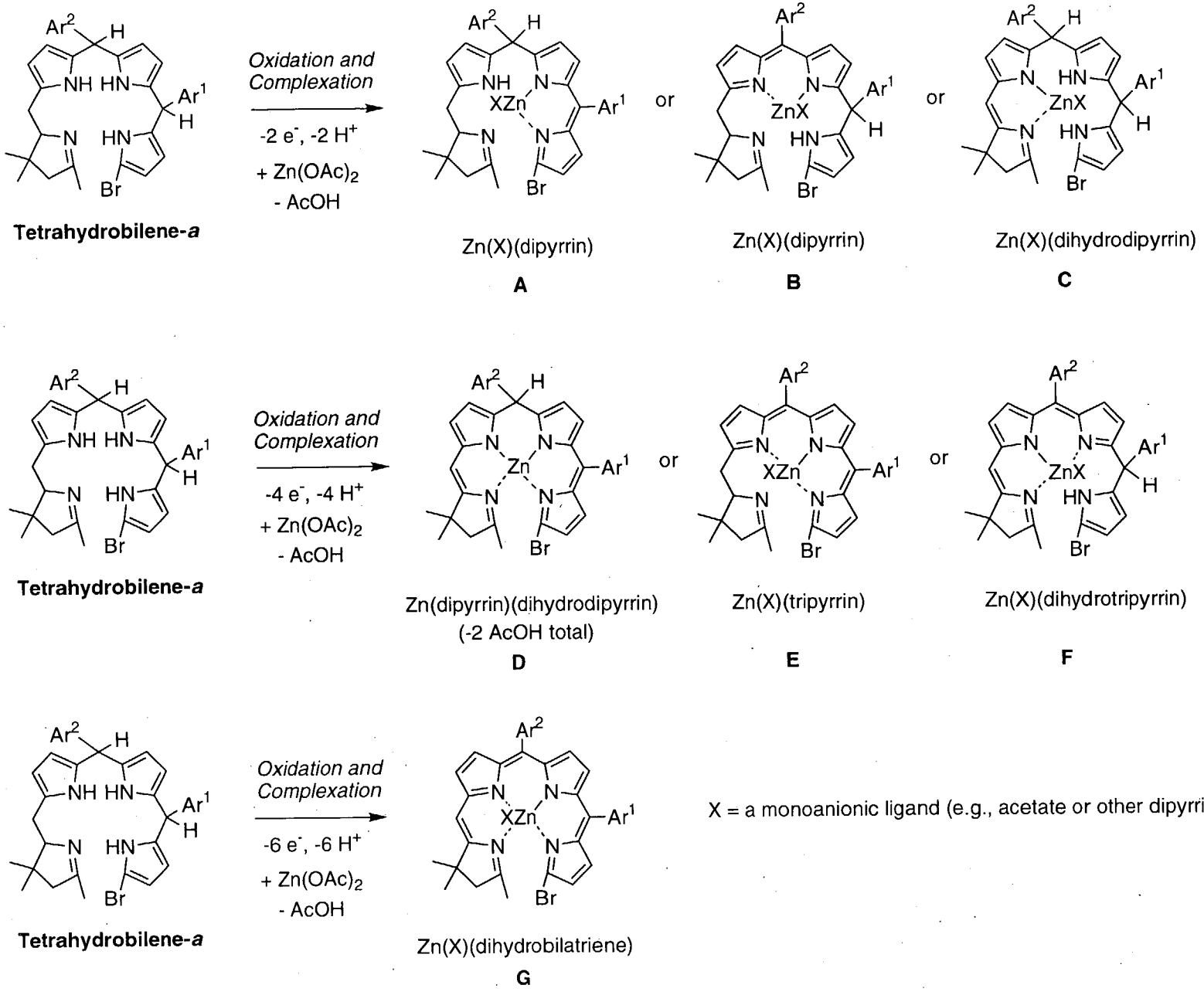

SI Scheme 2

SI Chart 1

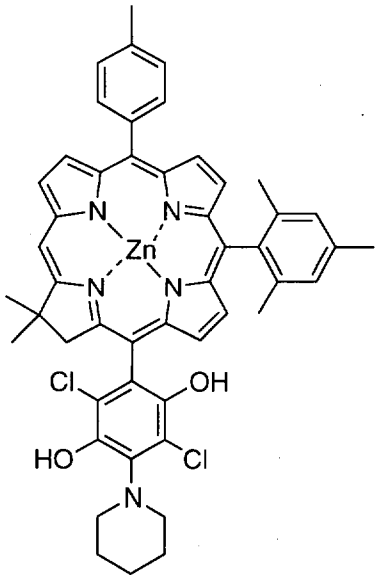

Zn-8a′

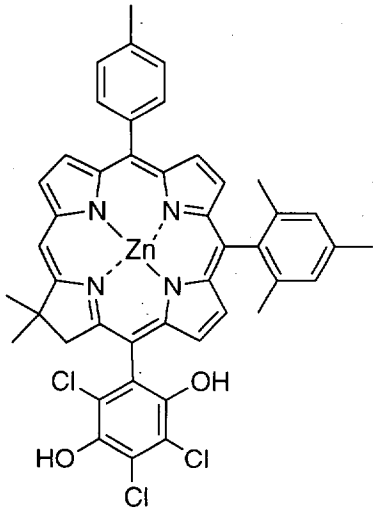

Zn-8a″

Nomenclature of acyclic tetrapyrromethanes

bilane:

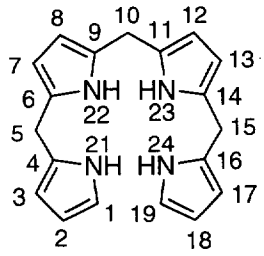

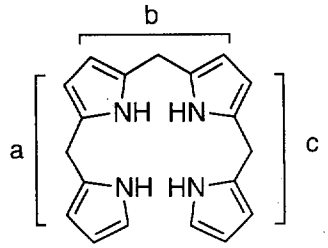

bilenes:

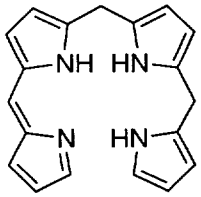

bilene-*a*

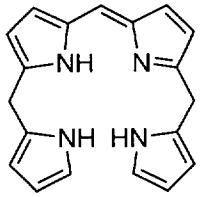

bilene-*b*

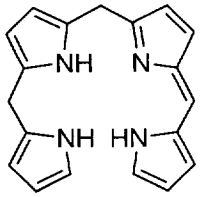

bilene-*c*

Hydrogenated bilin derivatives relevant to chlorin syntheses

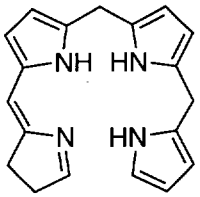

2,3-dihydrobilene-*a*

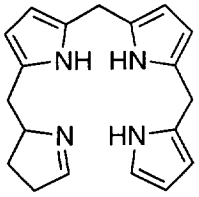

2,3,4,5-tetrahydrobilene-*a*

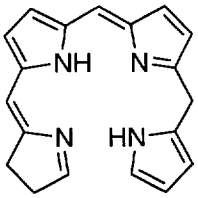

2,3-dihydrobiladiene-*ab*

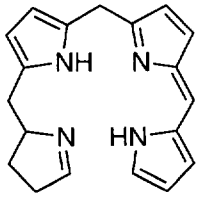

2,3,4,5-tetrahydrobiladiene-*ac*

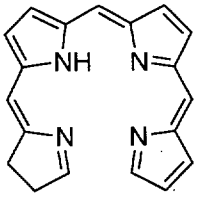

2,3-dihydrobilatriene

X-ray structural determination for the byproduct (5): 5,11-Diaza-1,9,9-trimethyltricyclo[6.2.1.$0^{2,6}$]undeca-2(6),3-diene.

Data Collection. The sample (NCSU number x01049), mounted on the end of a glass fiber using 5 minute epoxy, was transferred to the diffractometer. All X-ray measurements were made on an Enraf-Nonius CAD4 diffractometer at room temperature. The unit cell dimensions were determined by a symmetry-constrained fit of 25 well centered reflections and their Friedel pairs with theta 16° < 2(theta) < 29°. A unique quadrant of data was collected using theta/2theta scan mode. Three standard reflections were measured every 4800 seconds of X-ray exposure time. Scaling the data was accomplished using a 5 point smoothed curved routine fit to the intensity check reflections. The intensity data was corrected for Lorentz and polarization effects. An empirical absorption correction was applied using psi scan data.

Structure Solution and Refinement. The data were reduced using routines from the NRCVAX set of programs. The structure was solved using SIR92. All non-hydrogen atoms were refined anisotropically. Hydrogen atom positions were introduced at calculated positions, and were allowed to ride on the parent carbon or nitrogen atom. The hydrogen atom displacement parameters were also allowed to ride according to the following expression:

$U(H) = U_{eq}(\{C|N\}) + 0.01$.

The calculated structure factors were fit to the data using full matrix least-squares based on F. The calculated structure factors included corrections for anomalous dispersion from the usual tabulation (International Tables for X-ray Crystallography, Vol. IV, (1974), Table 2.3.1, Kynoch Press, Birmingham, England). A secondary extinction correction was included in the final cycles of refinement.

The ORTEP diagram, stereoscopic view, table of atomic parameters, and table of bond lengths and angles are included on the following pages.

Crystal Data Summary

Space Group and Cell Dimensions: Monoclinic, C 2/c
a 21.4201(14) b 7.8557(8) c 13.5494(12)
beta 94.288(13)
Volume: 2273.6(3)Å^3
Empirical formula: $C_{12}H_{18}N_2$
Cell dimensions were obtained from 25 reflections with 2Theta angle in the range 16.00 – 29.00°.
Crystal dimensions: 0.60 x 0.26 x 0.15 mm
FW = 190.29 Z = 8 F(000) = 832.41
D_{calc} = 1.112 Mg-m^{-3}, mu = 2.07 mm^{-1}, lambda = 0.71073Å, 2Theta(max) = 49.8°
The intensity data were collected on a Nonius diffractometer, using the theta/2theta scan mode.
The h,k,l ranges used during structure solution and refinement are as follows:
$H_{min,max}$ = -25 25; $K_{min,max}$ = 0 9; $L_{min,max}$ = 0 16

No. of reflections measured	1992
No. of unique reflections	1992
No. of reflections with Inet > 1.0sigma(Inet)	1992
Merging R-value on intensities	.000

The last least squares cycle was calculated with 32 atoms, 200 parameters and 1992 out of 1992 reflections.

Weights based on counting-statistics were used.
The weight modifier K in KF_o^2 is 0.000500
The residuals are as follows:

For significant reflections, R_F 0.061; R_w 0.070; GoF 1.88
For all reflections, R_F 0.061, R_w 0.070.
where $R_F = Sum(F_o-F_c)/Sum(F_o)$,
$R_w = Sqrt[Sum(w(F_o-F_c)^2)/Sum(wF_o^2)]$ and
$GoF = Sqrt[Sum(w(F_o-F_c)^2)/(No.\ of\ reflns - No.\ of\ params.)]$

The maximum shift/sigma ratio was 0.000.
In the last D-map, the deepest hole was $-0.200e/Å^3$, and the highest peak $0.180e/Å^3$.
Secondary ext. coeff. 0.8166 microns, sigma 0.0429

The following references are relevant to the NRCVAX System.

(1) Full System Reference: Gabe, E. J.; Le Page, Y.,; Charland,.J.-P.; Lee, F. L.; White, P.S. *J. Appl. Cryst.* **1989**, *22*, 384-387.
(2) Scattering Factors: *International Tables for X-ray Crystallography*, 1974, Vol. IV, Kynoch Press: Birmingham, England.
(3) Extinction Treatment: Larson, A. C. *Crystallographic Computing*, 1970 Munksgaard: Copenhagen, p. 293.
(4) Reference for SIR92: Altomare, A.; Burla, M. C.; Camalli, G.; Cascarano, G.; Giacovazzo, C.; Guagliardi, A.; Polidori, G. *J. Appl. Cryst.* **1994**, *27*, 435-436.
(5) Reference for Psi-scans: North, A. C. T.; Phillips, D. C.; Mathews, F.S. *Acta Cryst.* **1968**, *A24*, 351-359.

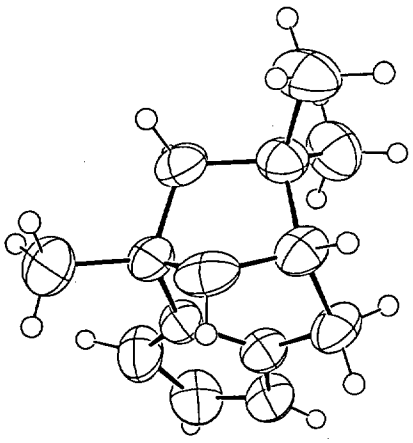

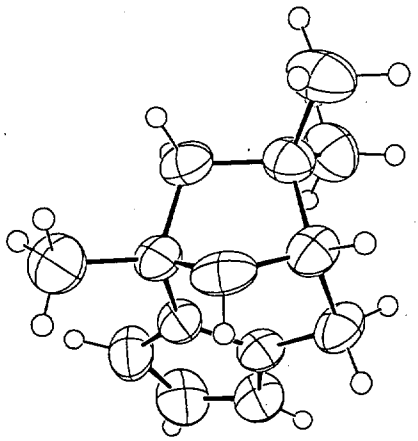

X01049: ROOM TEMP

3-May-2001

Table . Atomic Parameters x,y,z and Biso.
E.S.Ds. refer to the last digit printed.

	x	y	z	Biso
N1	.42167(7)	.1344(2)	.66189(10)	4.91(8)
N2	.41734(7)	-.0125(2)	.37127(9)	4.82(8)
C1	.41026(7)	.0700(2)	.56804(10)	3.92(7)
C2	.39286(11)	-.1076(2)	.53965(12)	4.83(10)
C3	.37203(8)	-.1075(2)	.42782(11)	4.45(9)
C4	.30992(8)	-.0119(2)	.39738(11)	4.47(8)
C5	.33269(9)	.1641(3)	.36501(13)	4.66(9)
C6	.40307(8)	.1676(2)	.39283(10)	4.14(8)
C7	.41594(7)	.1989(2)	.50265(10)	3.84(7)
C8	.43041(9)	.3481(3)	.55795(13)	5.66(10)
C9	.43355(9)	.3035(3)	.65502(14)	6.01(11)
C10	.26519(11)	.0046(4)	.48005(17)	6.23(12)
C11	.27499(13)	-.1058(4)	.31028(18)	6.65(13)
C12	.43826(15)	.2933(5)	.33147(16)	7.50(15)
H1	.4186 (8)	.076 (2)	.7185 (13)	7.0 (5)
H2	.4556 (7)	-.0390(20)	.3949 (12)	5.5 (5)
H2a	.4303 (8)	-.185 (2)	.5518 (12)	6.1 (5)
H2b	.3582 (8)	-.1529(19)	.5755 (13)	6.0 (5)
H3	.3707 (6)	-.2296(20)	.4036 (11)	4.9 (4)
H8	.4334 (7)	.462 (2)	.5319 (12)	6.1 (4)
H5a	.3252 (7)	.1786(18)	.2936 (12)	5.3 (4)
H5b	.3109 (7)	.2586(20)	.3976 (11)	5.3 (4)
H9	.4437 (8)	.371 (2)	.7148 (13)	6.9 (5)
H10a	.2543 (9)	-.112 (3)	.5018 (15)	8.7 (6)
H10b	.2857 (8)	.076 (2)	.5390 (14)	7.2 (5)
H10c	.2268 (10)	.063 (3)	.4531 (16)	10.0 (7)
H11a	.3020 (9)	-.125 (2)	.2587 (14)	6.8 (5)
H11b	.2374 (10)	-.036 (3)	.2863 (15)	9.2 (6)
H11c	.2586 (9)	-.230 (3)	.3354 (14)	8.7 (6)
H12a	.4226 (13)	.408 (4)	.333 (2)	15.0 (13)
H12b	.4284 (9)	.265 (2)	.2635 (17)	8.5 (5)
H12c	.4827 (12)	.279 (3)	.3447 (17)	11.7 (9)

Biso is the Mean of the Principal Axes of the Thermal Ellipsoid

Table of u(i,j) or U values *100.
E.S.Ds. refer to the last digit printed

	u11(U)	u22	u33	u12	u13	u23
N1	7.96(11)	7.88(13)	2.77(8)	-.76(9)	.20(7)	-.11(8)
N2	5.69(10)	9.46(13)	3.08(7)	1.64(10)	-.14(7)	-.72(8)
C1	5.95(11)	6.11(11)	2.76(8)	-.13(9)	-.12(7)	-.24(8)
C2	8.29(15)	5.86(13)	4.04(10)	.32(12)	-.51(10)	.45(9)
C3	7.45(13)	5.35(12)	4.01(10)	.46(10)	-.29(9)	-.69(9)
C4	5.75(11)	6.46(12)	4.68(9)	-.28(10)	-.30(8)	-.42(9)
C5	6.24(12)	7.19(14)	4.13(10)	.53(11)	-.56(9)	.64(10)
C6	5.76(11)	6.78(12)	3.15(8)	-.34(9)	.11(8)	.64(8)
C7	5.55(11)	5.86(11)	3.17(8)	-.59(9)	.22(7)	.11(8)
C8	9.75(16)	6.53(14)	5.08(12)	-2.23(12)	-.33(10)	.24(11)
C9	10.12(16)	7.82(16)	4.80(12)	-1.77(13)	.00(10)	-1.94(12)
C10	7.63(16)	8.53(18)	7.68(15)	-.97(15)	1.70(13)	-.72(14)
C11	7.84(16)	10.4 (2)	6.65(14)	-1.20(15)	-1.50(13)	-1.75(14)
C12	9.6 (2)	14.7 (3)	4.14(12)	-3.26(19)	.37(12)	2.98(15)
H1	8.9(6)					
H2	6.9(6)					
H2a	7.8(6)					
H2b	7.6(6)					
H3	6.2(5)					
H8	7.7(6)					
H5a	6.7(5)					
H5b	6.7(5)					
H9	8.7(6)					
H10a	11.1(8)					
H10b	9.1(6)					
H10c	12.6(9)					
H11a	8.6(7)					
H11b	11.7(8)					
H11c	11.0(8)					
H12a	19.0(17)					
H12b	10.8(7)					
H12c	14.8(11)					

Anisotropic Temperature Factors are of the form
Temp=-2*Pi*Pi*(h*h*u11*astar*astar+---+2*h*k*u12*astar*bstar+---)

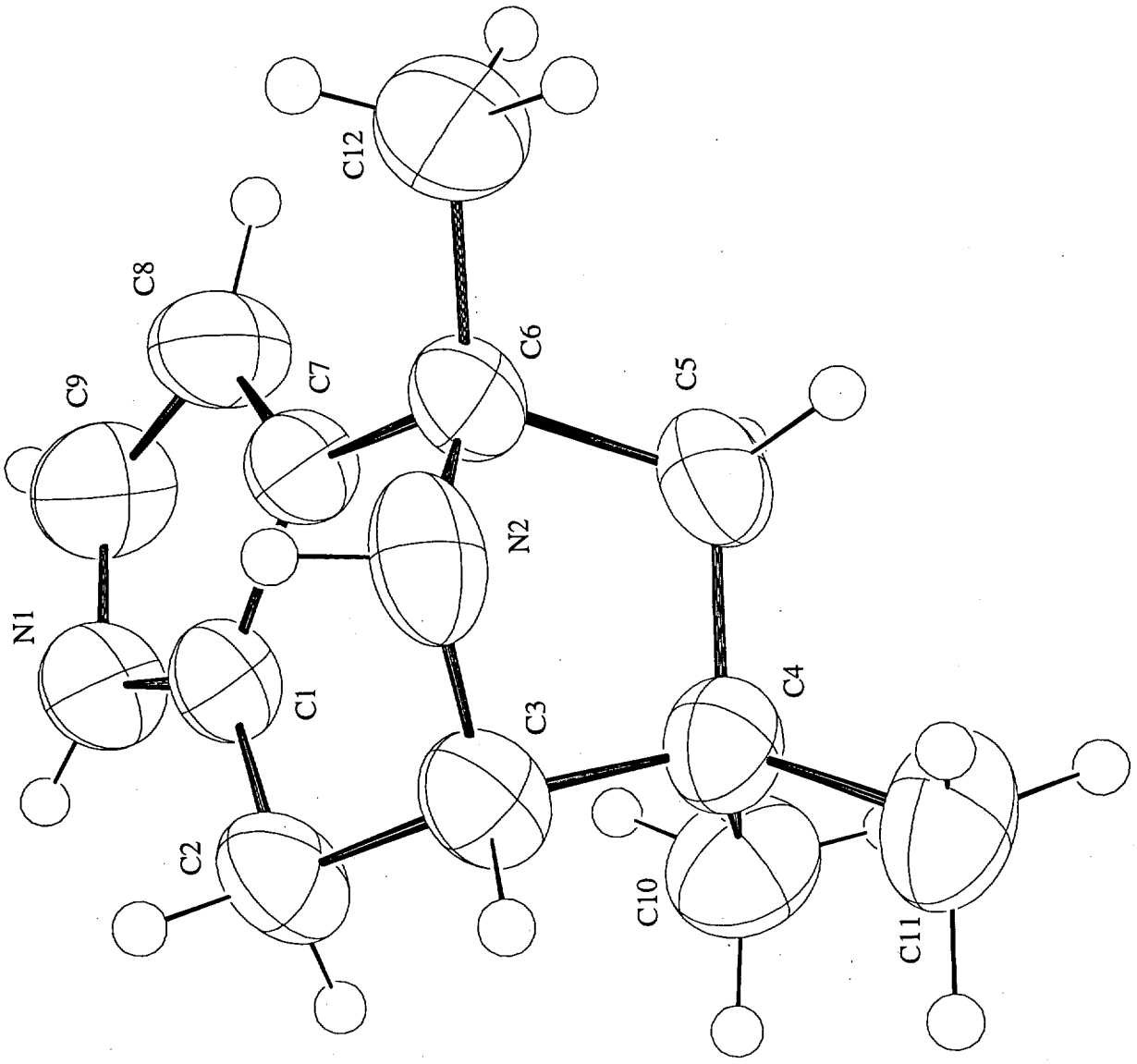
C12
C8
C9
C7
C6
C5
N2
N1
C1
C3
C4
C2
C10
C11

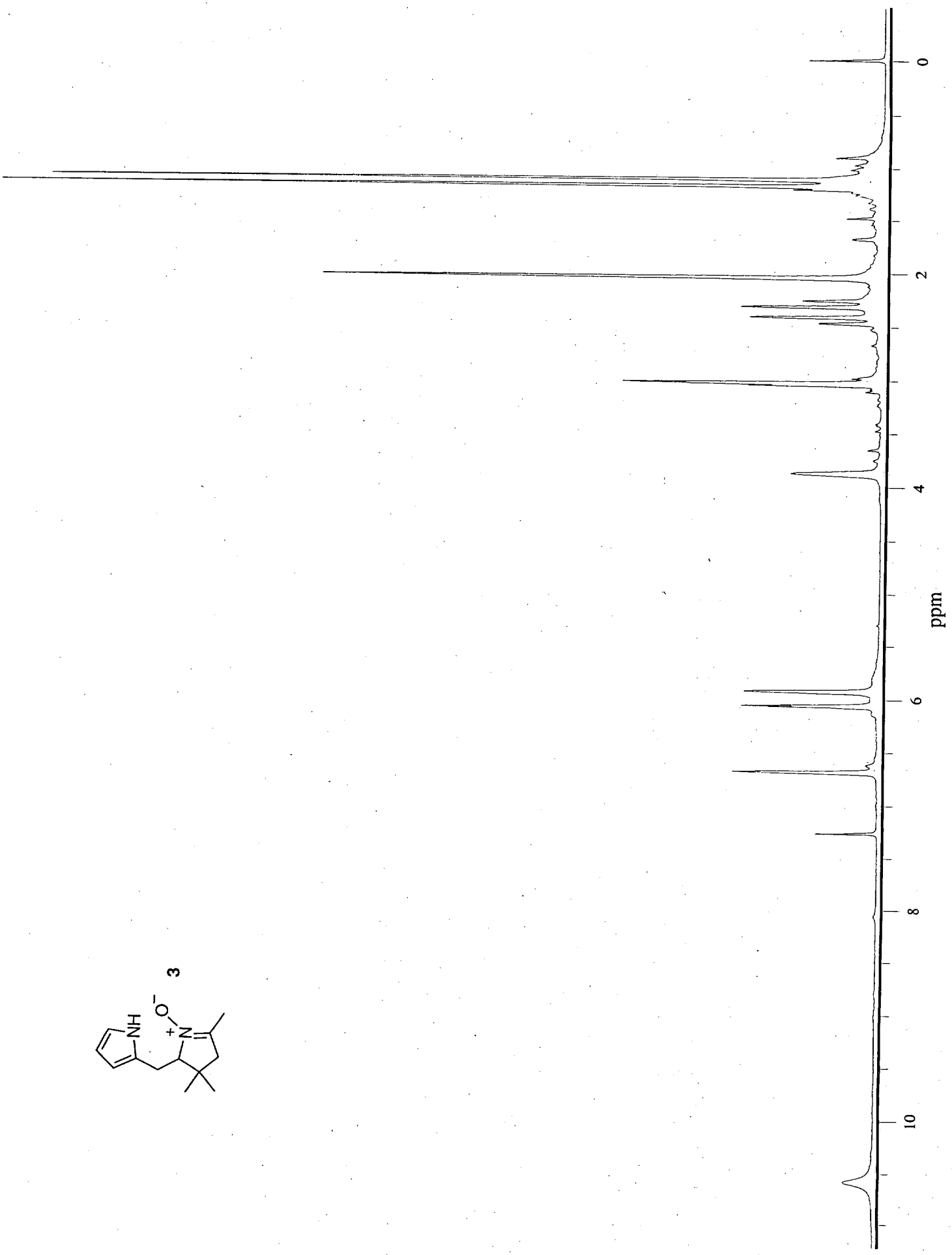

3

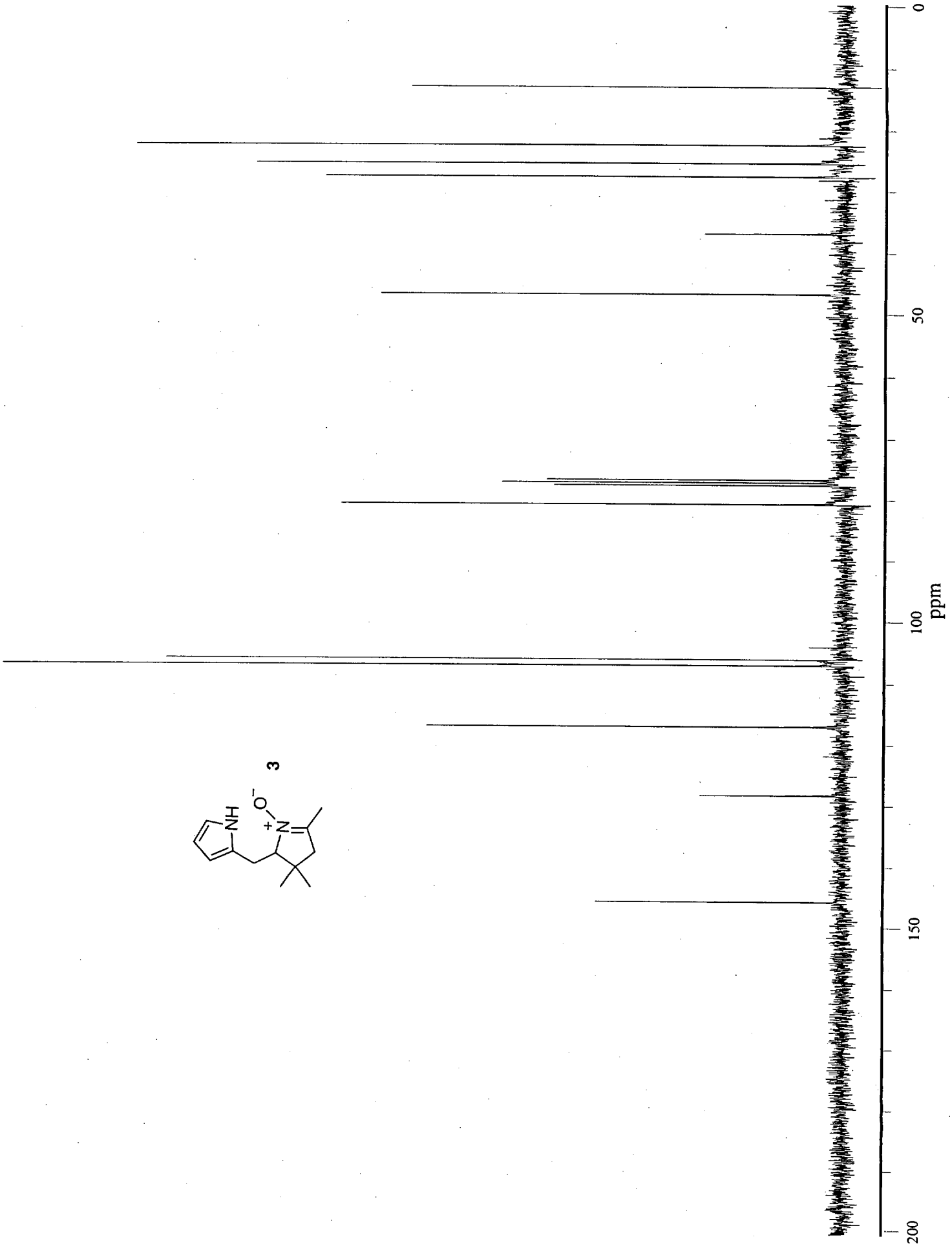

3

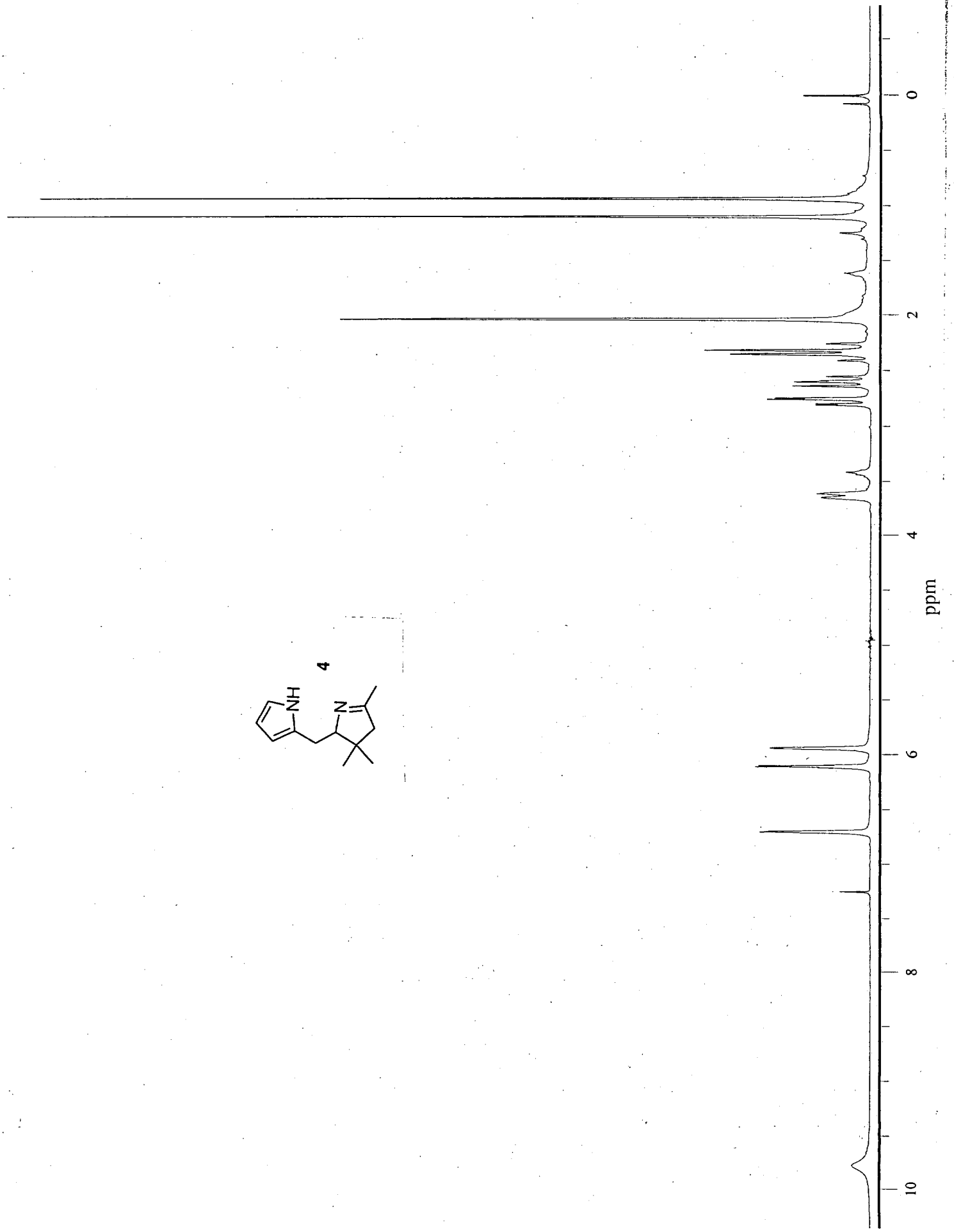

4

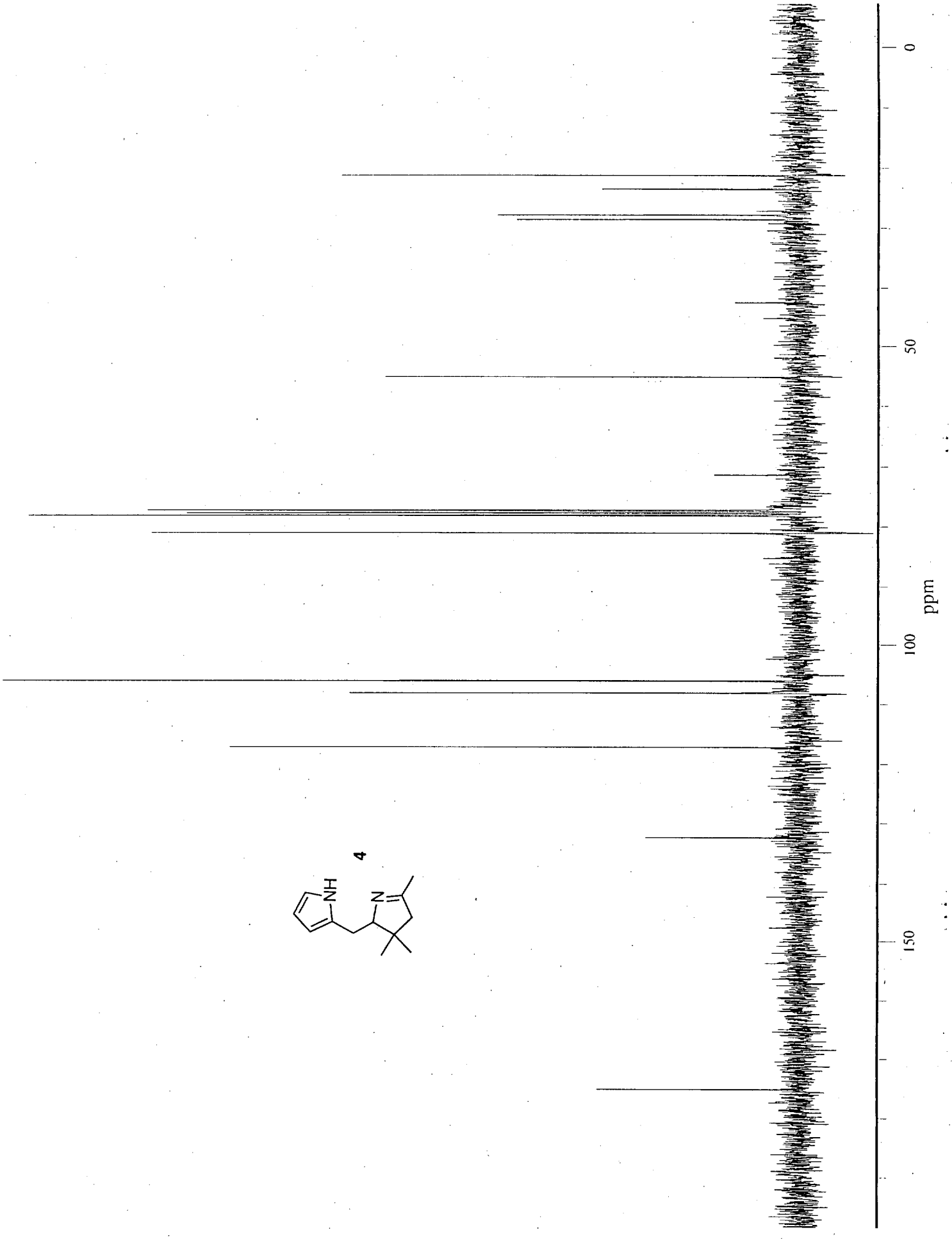

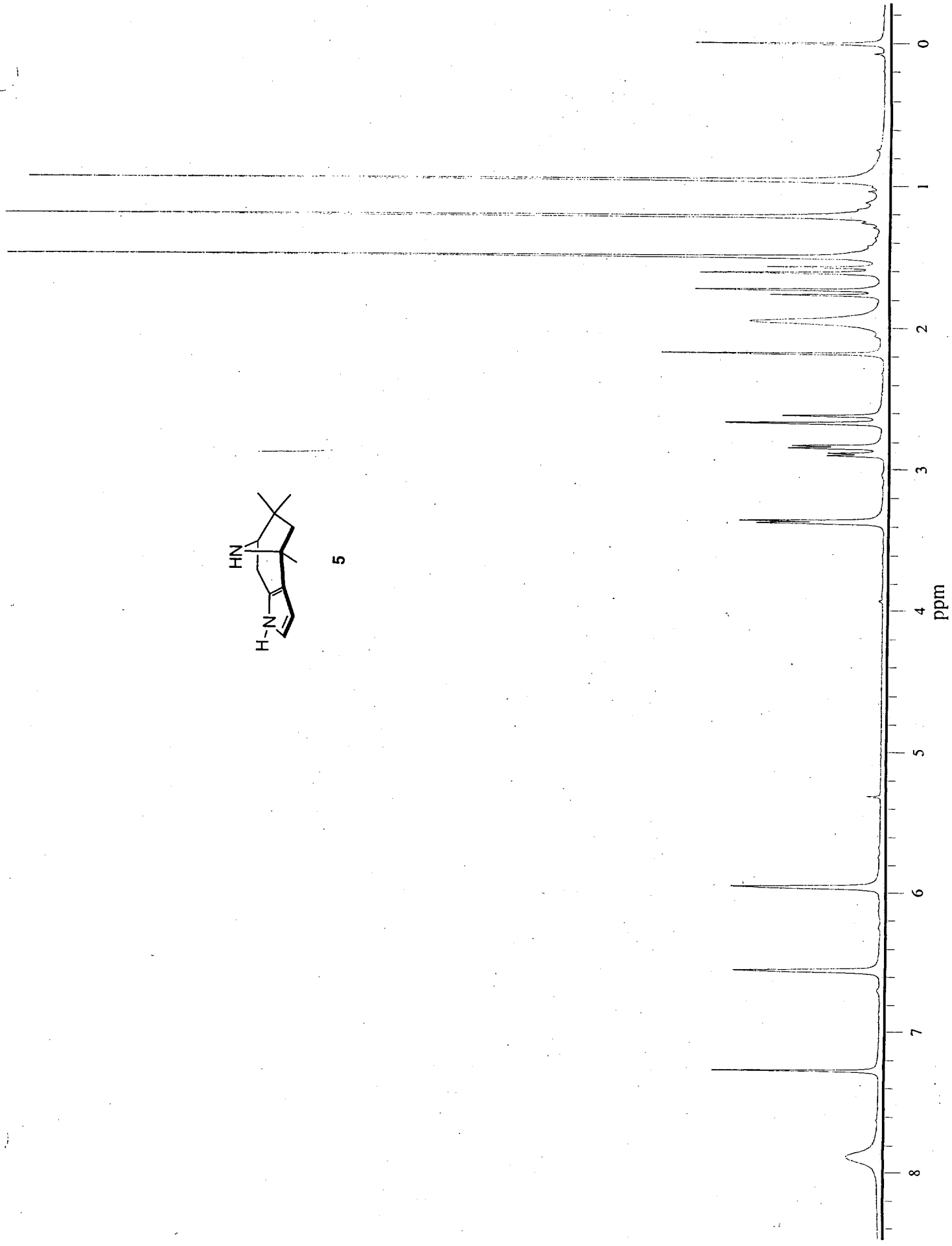

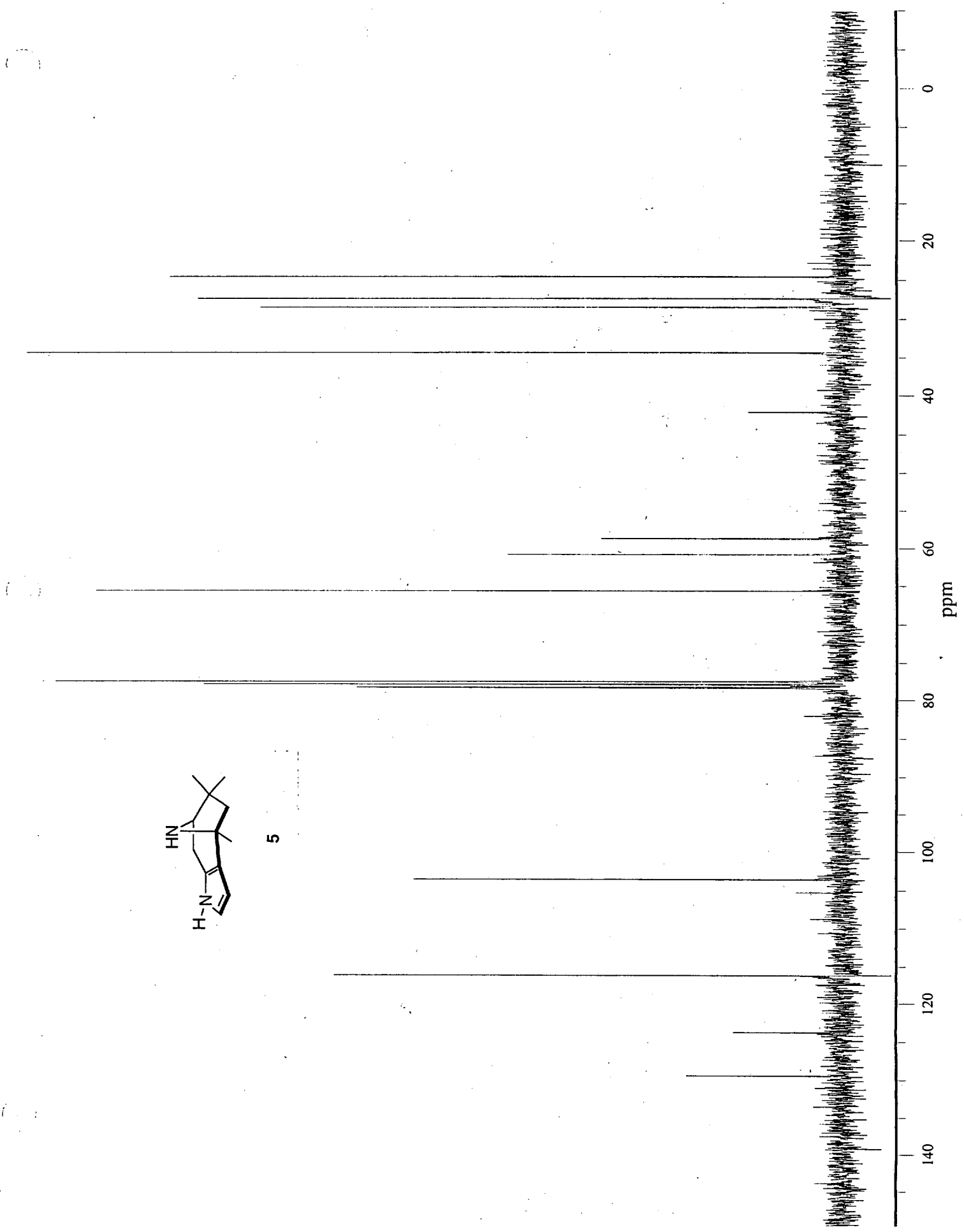

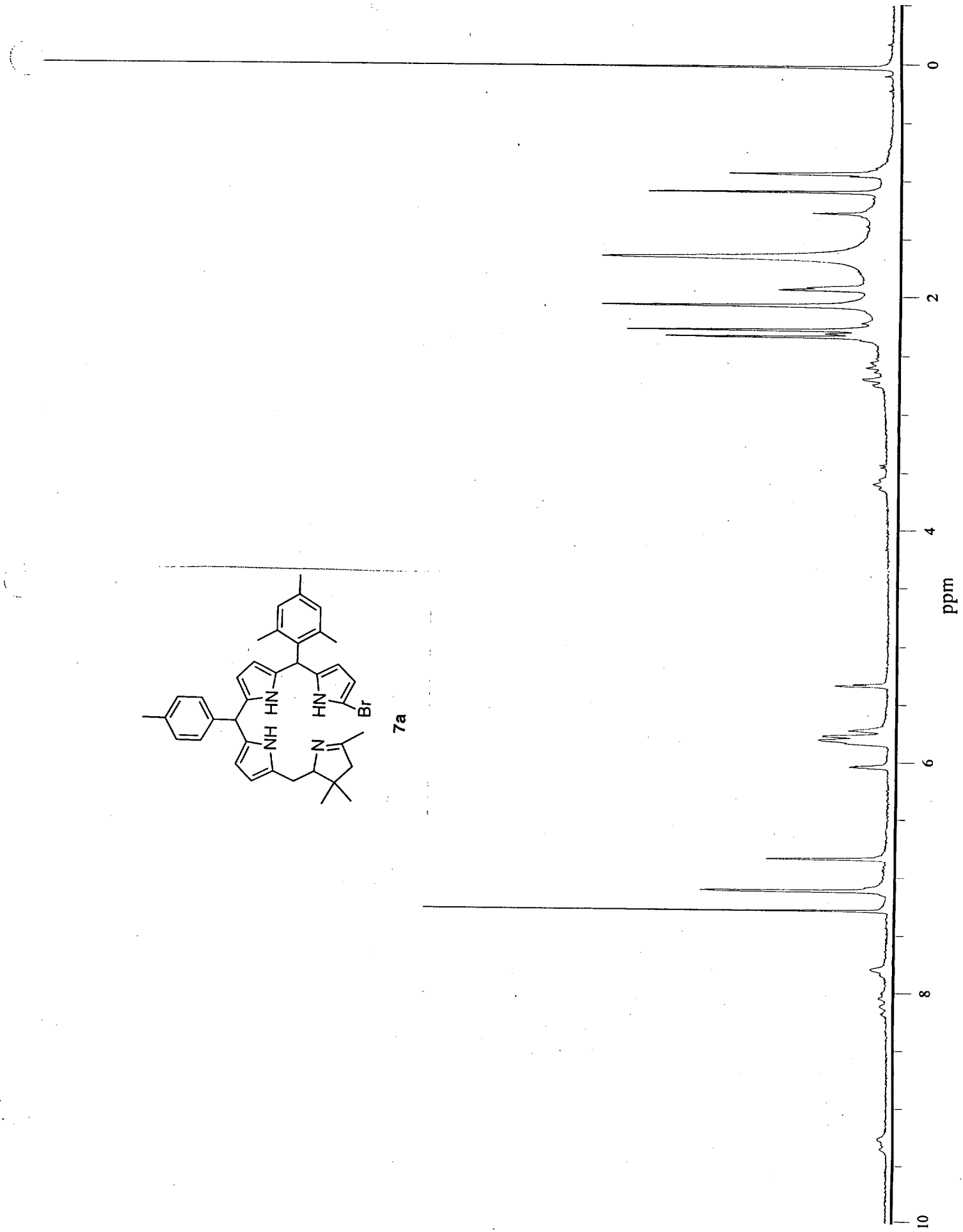

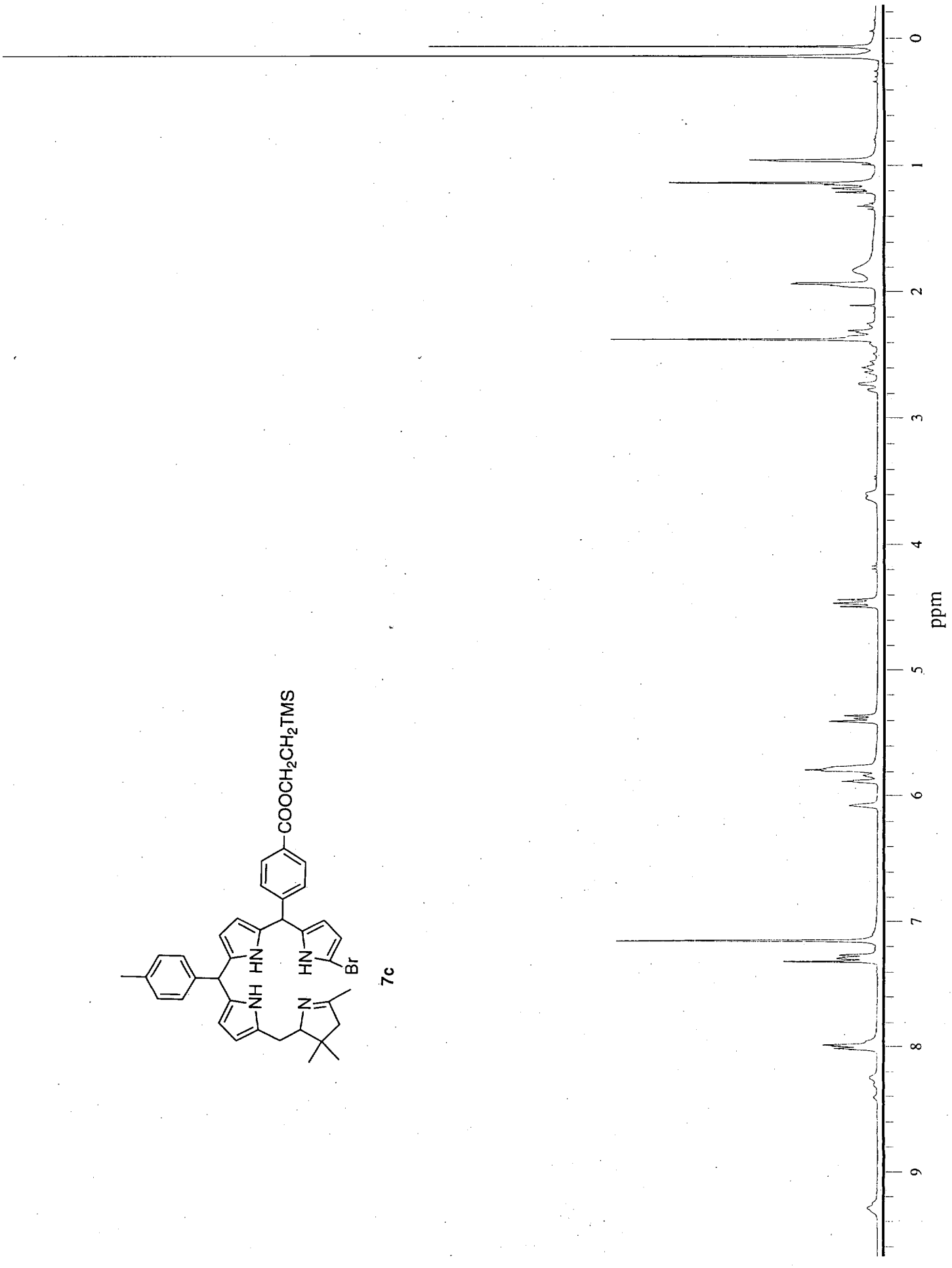

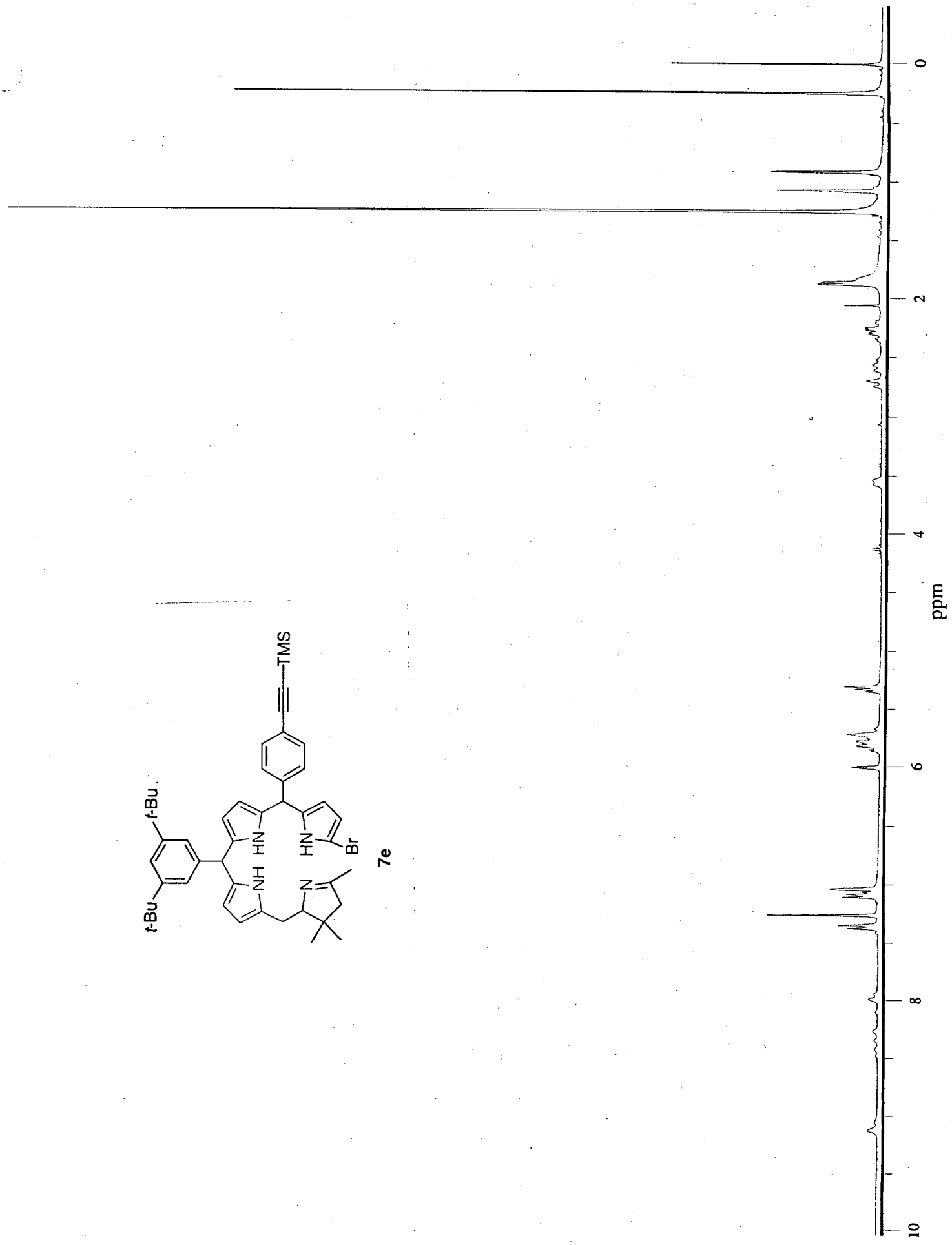

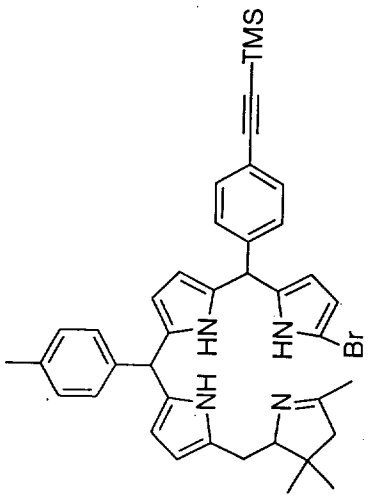

7f

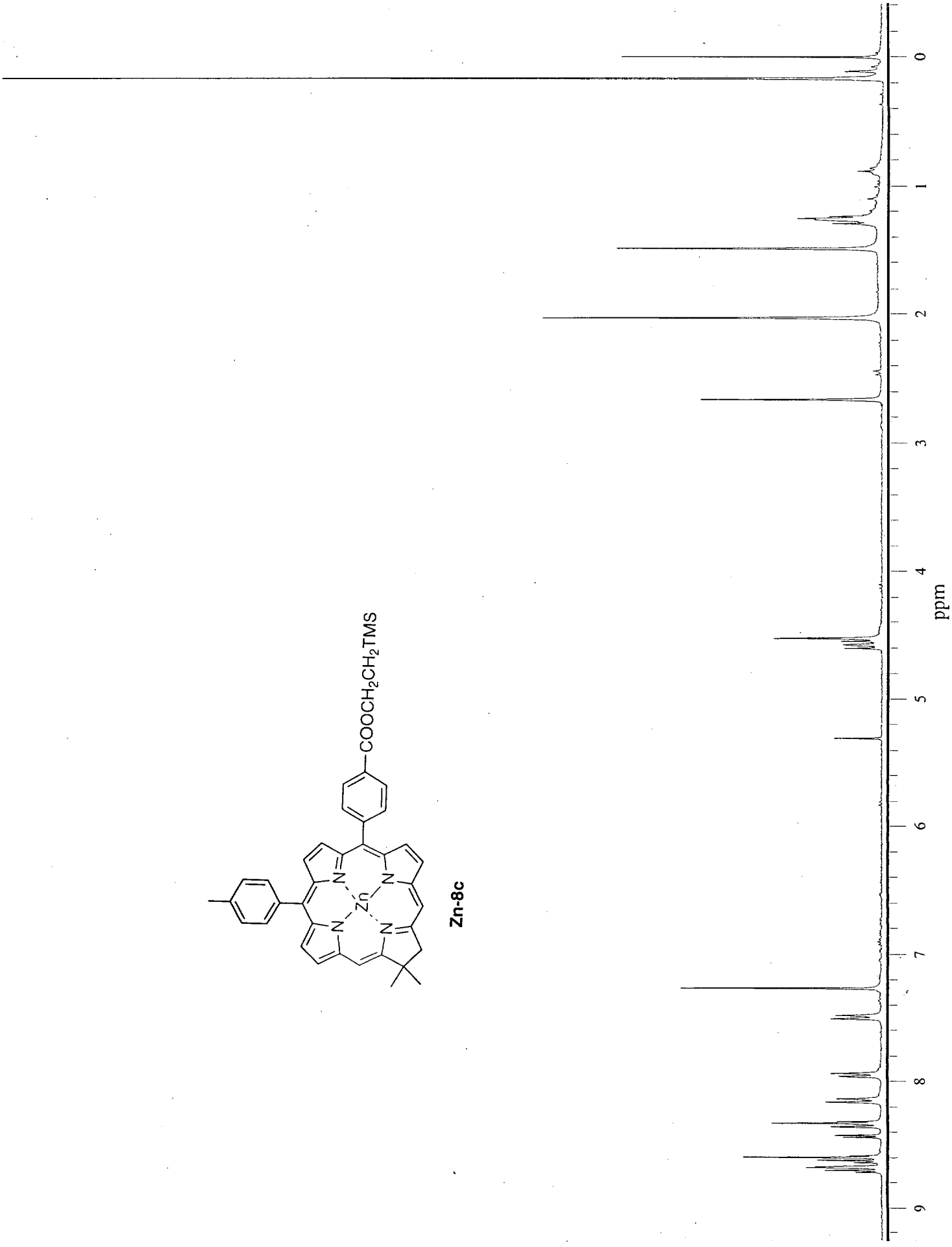
COOCH2CH2TMS
Zn
N
N
N
N
Zn-8c
0
1
2
3
4
5
6
7
8
9
ppm

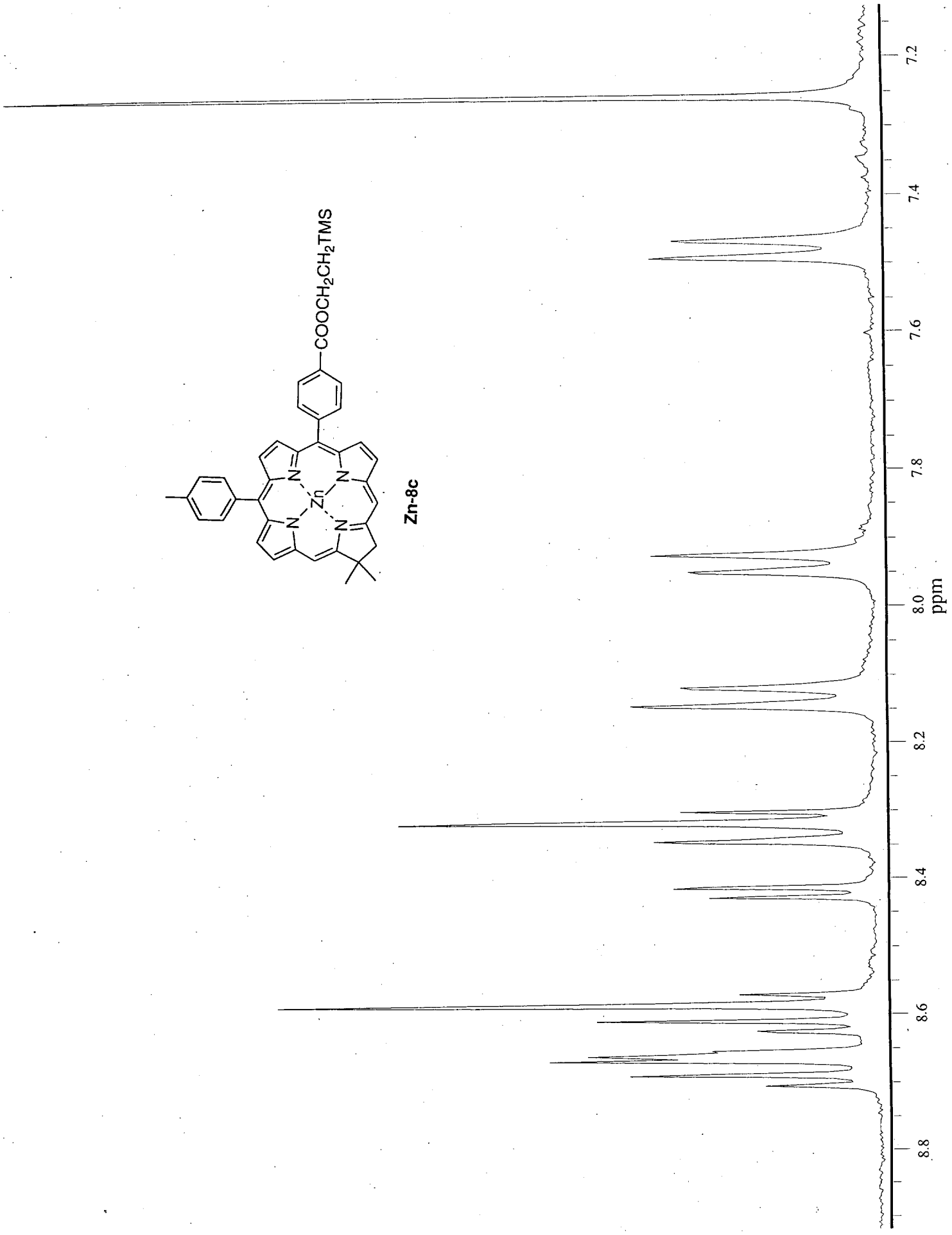

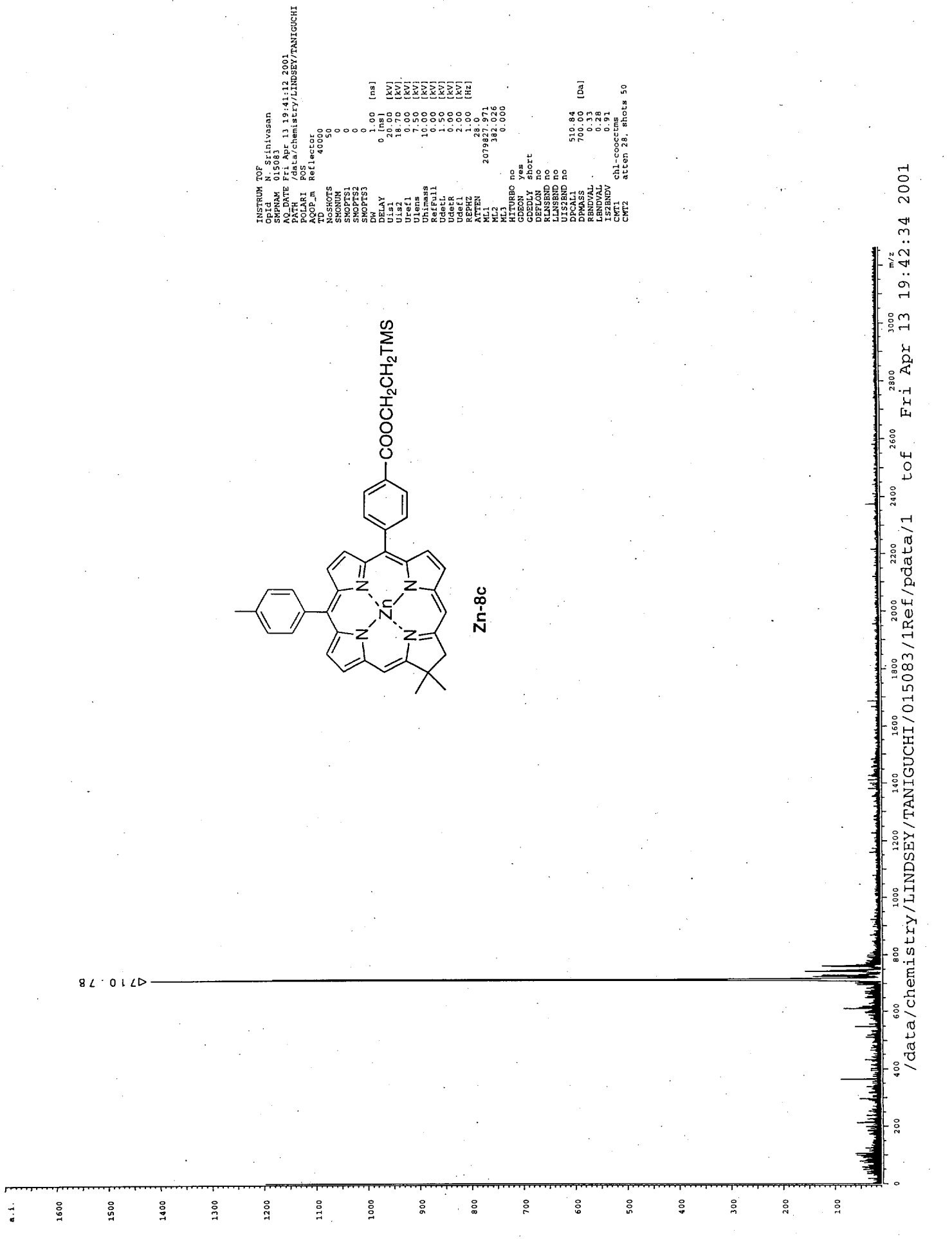

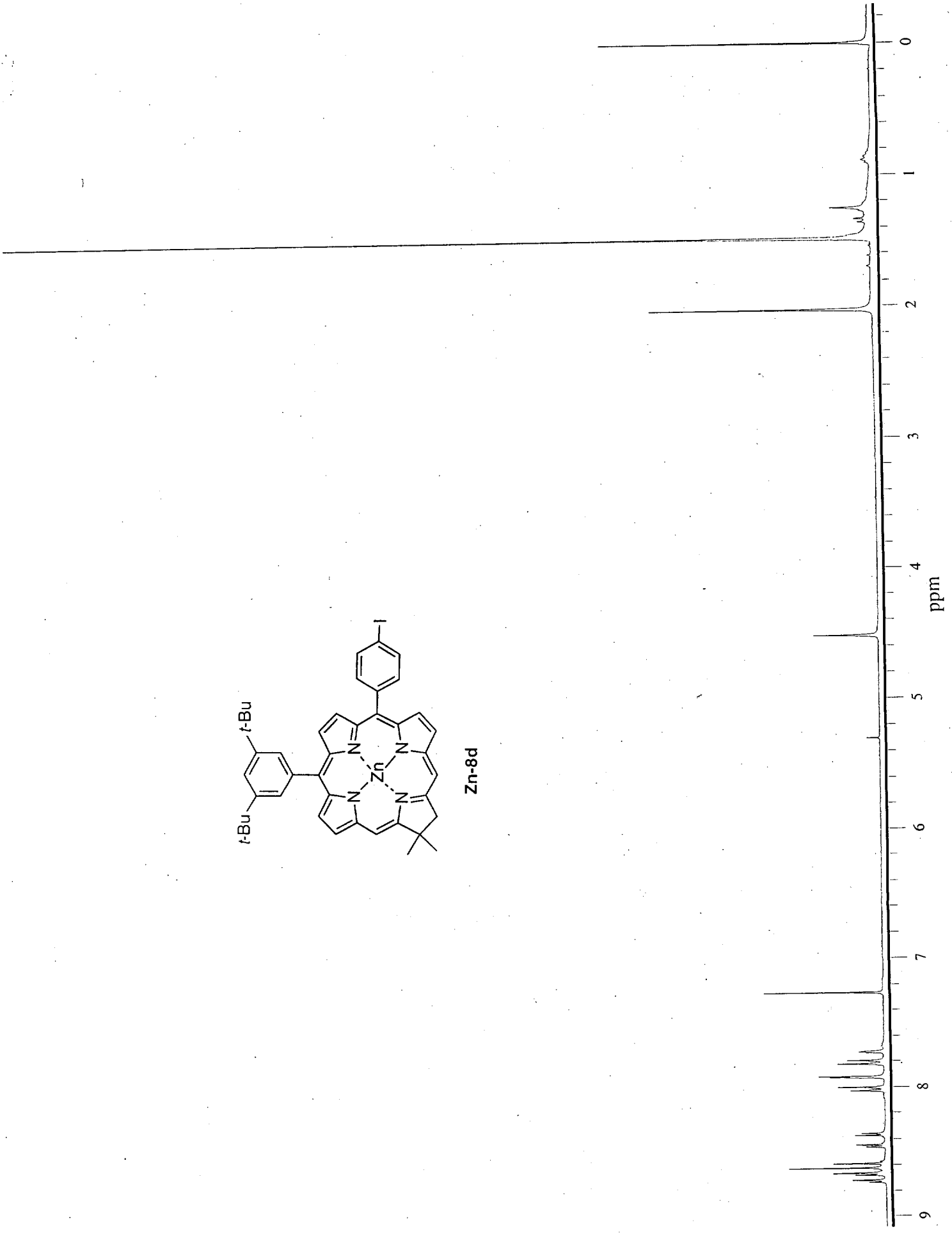

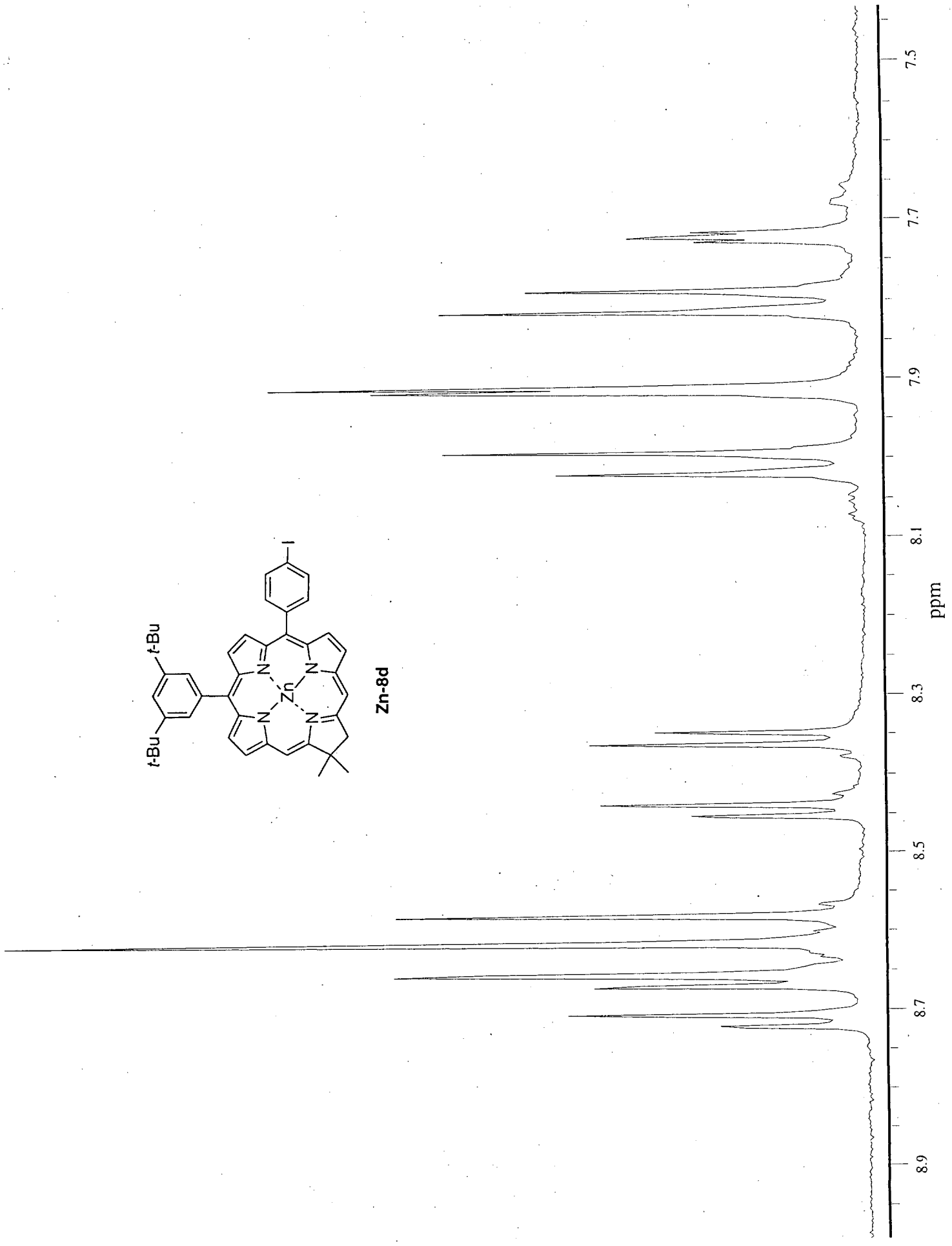

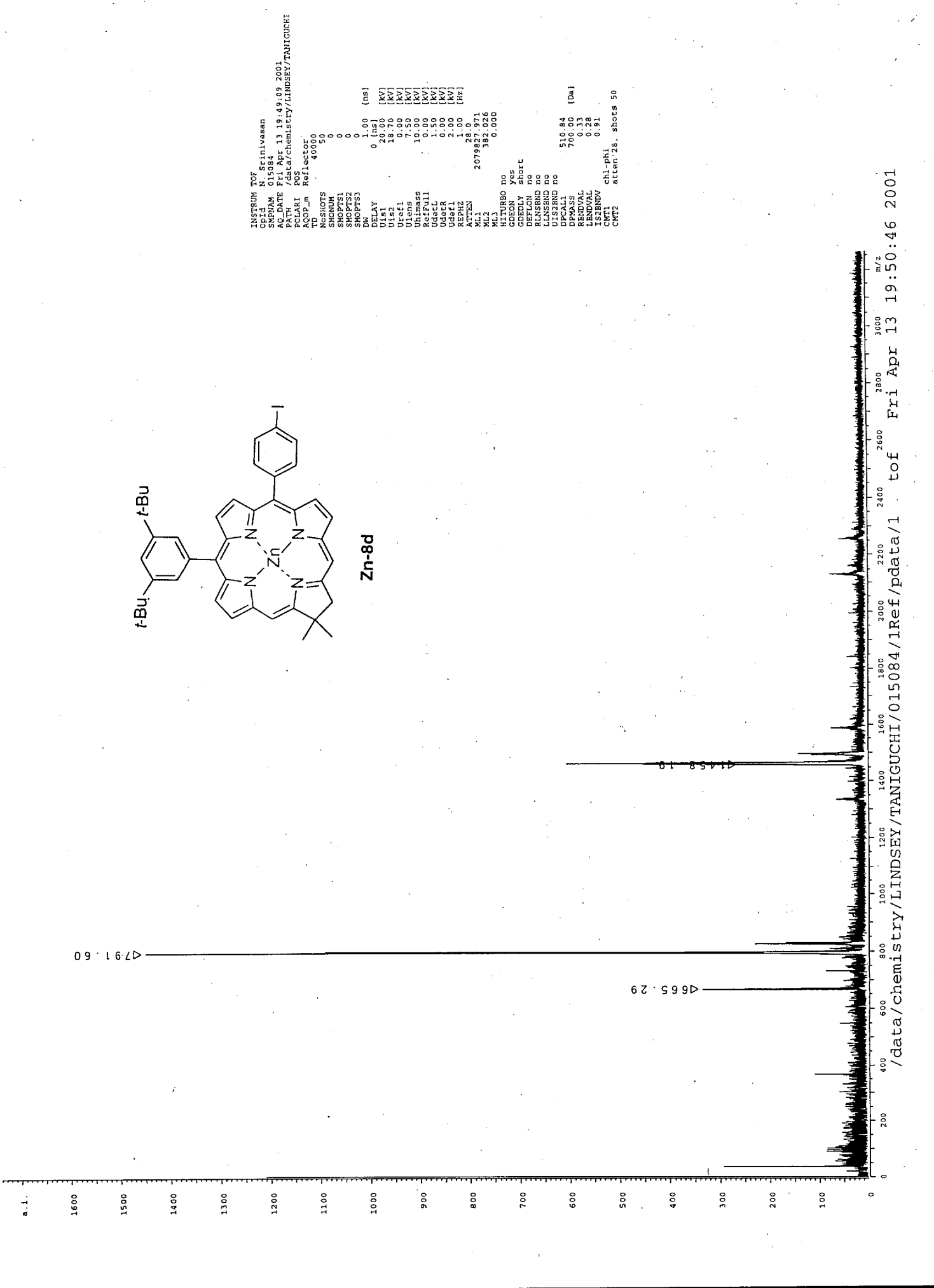

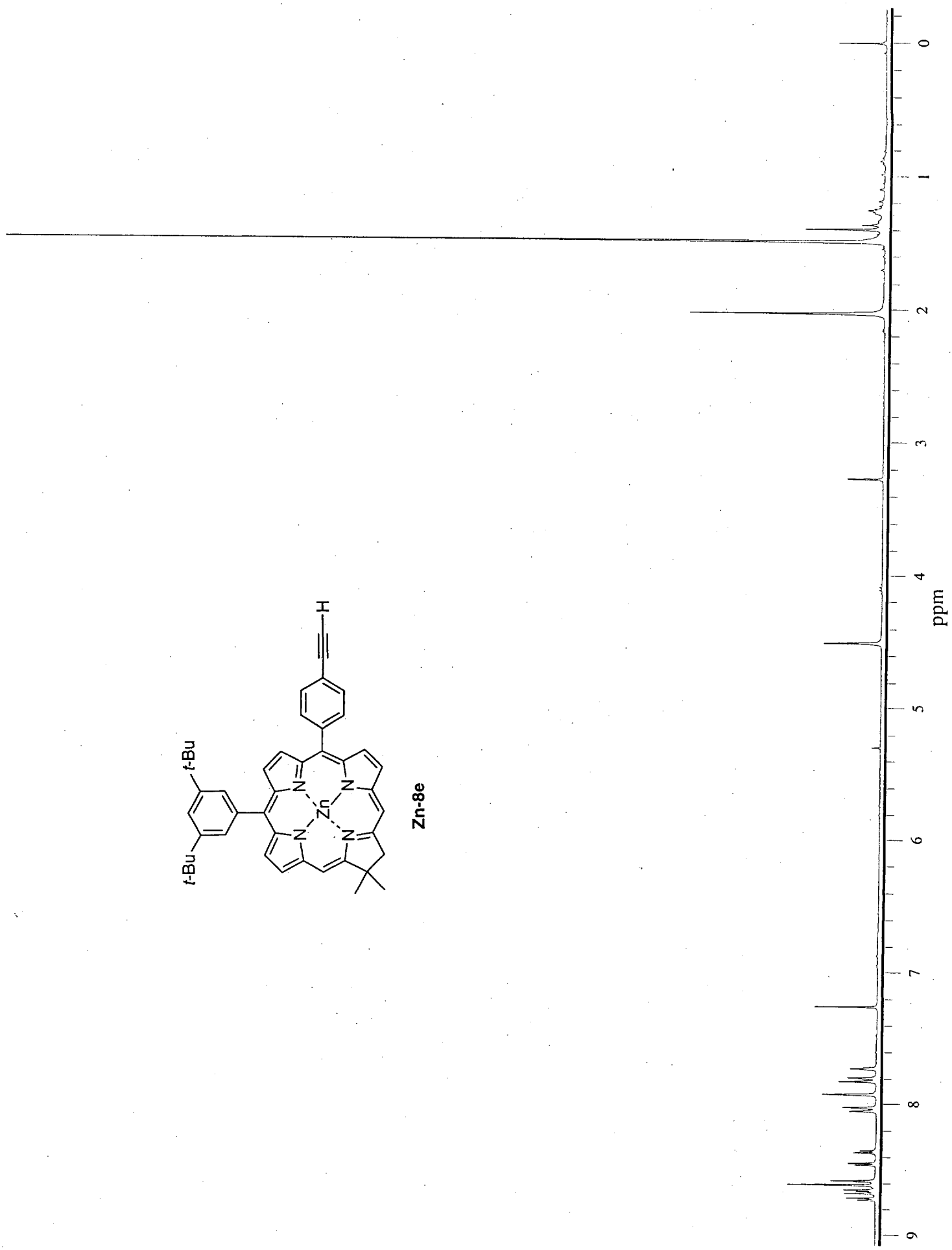

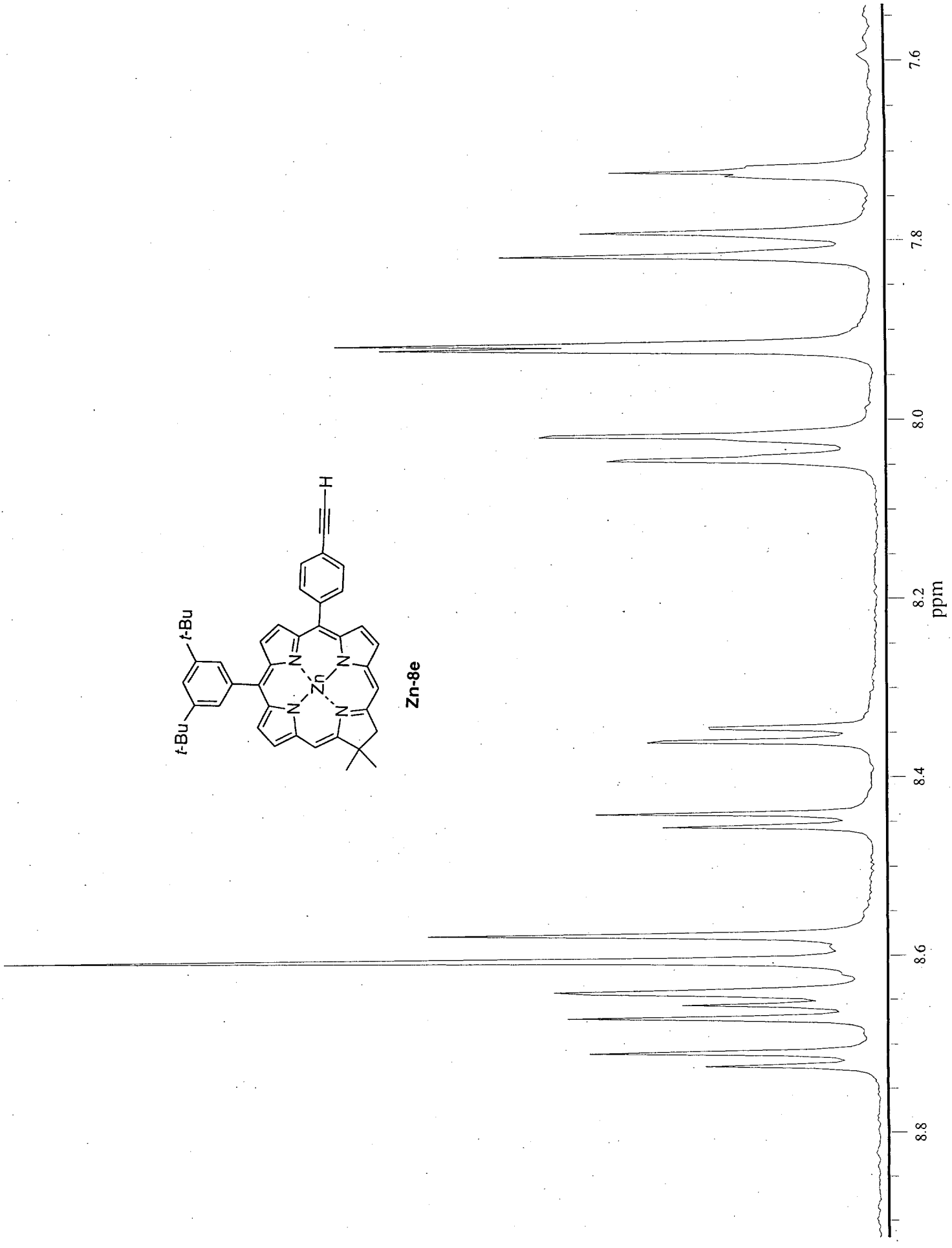
t-Bu
t-Bu
H
N
N
N
N
Zn
Zn-8e
7.6
7.8
8.0
8.2
8.4
8.6
8.8
ppm

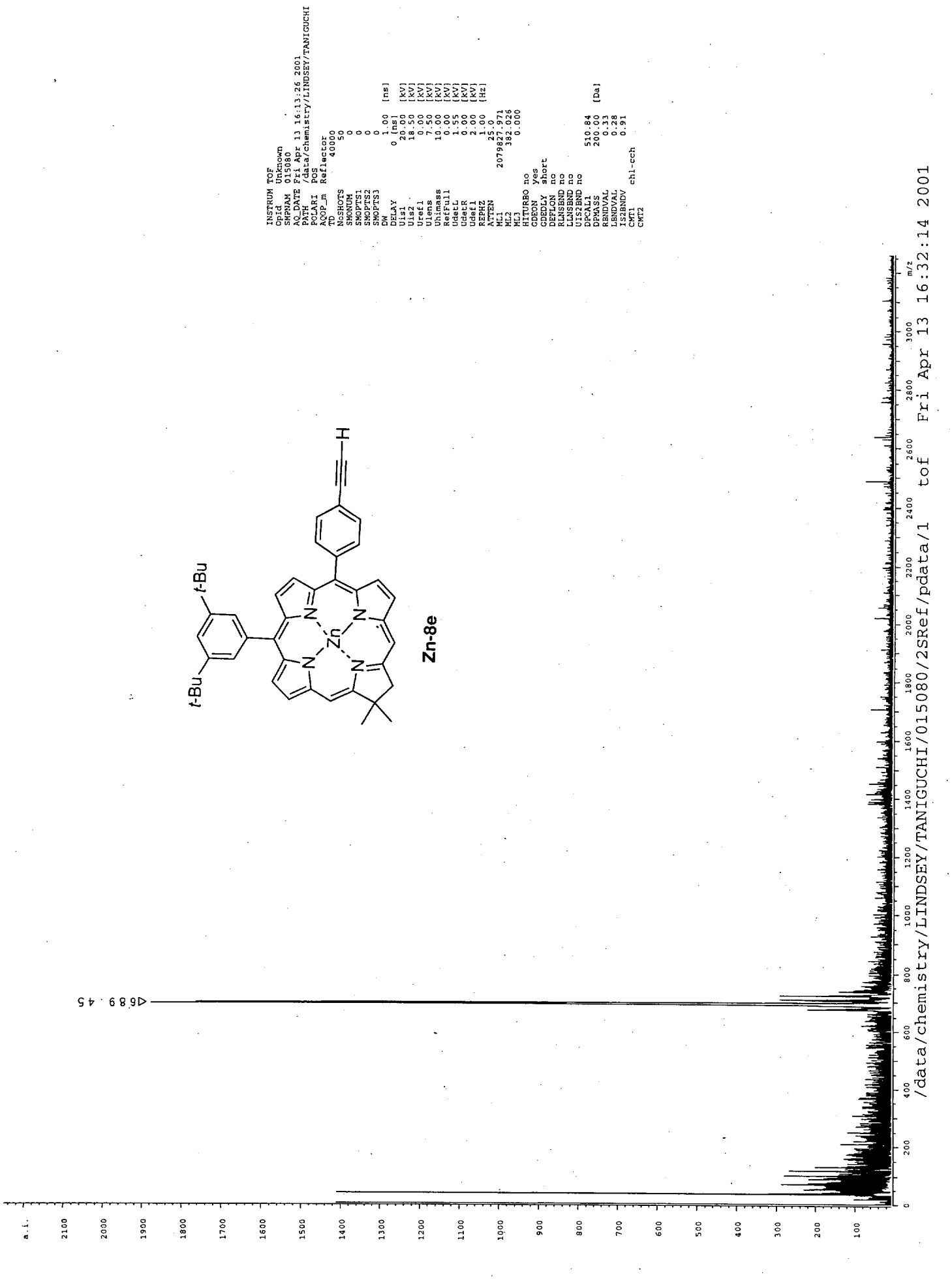

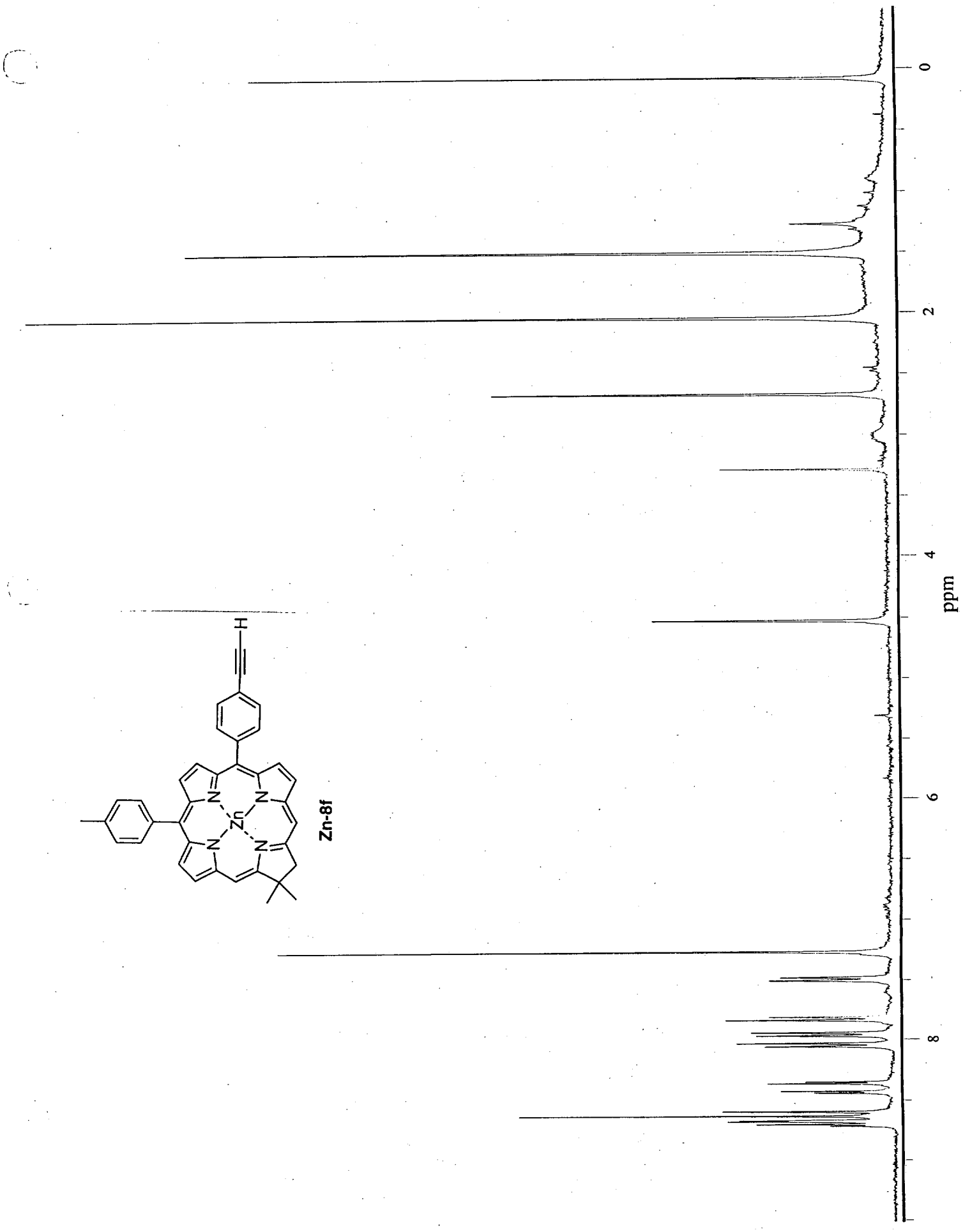

Zn-8f

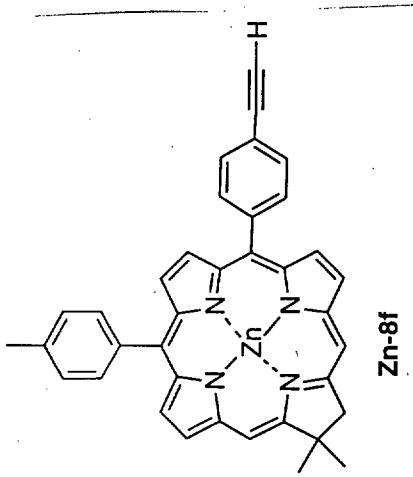

Zn-8f